Matroid Method versus Tsai-Tokad (T-T) Graph Method in the Kinematic Analysis of the Mechanical Systems consisting of Gears

Seyedvahid Amirinezhad

Submitted to the
Institute of Graduate Studies and Research
In partial fulfillment of the requirements for the Degree of

Master of Science
in
Electrical and Electronic Engineering

Eastern Mediterranean University
December 2013
Gazimağusa, North Cyprus

Approval of the Institute of Graduate Studies and Research

Prof. Dr. Elvan Yılmaz
Director

I certify that this thesis satisfies the requirements as a thesis for the degree of Master of Science in Electrical and Electronic Engineering.

Prof. Dr. Aykut Hocanın
Chair, Department of Electrical and Electronic Engineering

We certify that we have read this thesis and that in our opinion it is fully adequate in scope and quality as a thesis for the degree of Master of Science in Electrical and Electronic Engineering.

Assoc. Prof. Dr. Mustafa Kemal Uyguroğlu
Supervisor

Examining Committee

1. Prof. Dr. Osman Kükrer _____

2. Assoc. Prof. Dr. Hasan Demirel _____

3. Assoc. Prof. Dr. Mustafa Kemal Uyguroğlu _____

ABSTRACT

In this thesis, Matroid and T-T Graph methods are compared. These are graphical methods which are used in kinematic analysis of mechanisms including gear trains. Both methods are based on Graph Theory. T-T graph method is developed by combining non-oriented graphs and oriented graphs. Whereas, incident matrix derived from oriented graph is used in Matroid. In order to perform kinematic analysis by using these two methods, a conventional Geared Robotic Mechanism (GRM) is considered as a sample mechanism.

In Matroid, depending on the numbering links and joints, the digraph attached to kinematic chains is generated. Reduced incidence node-edge, spanning tree, path and cycle basis matrices are developed for this digraph. Equations for relative angular velocities of all turning and gear pairs are defined. Screw theory and plücker coordinates are defined to find the offset angles betwen z-axes of joints and z-axis of base. Twist intensities matrix is produced for turning and meshing pairs. Orthogonality condition for relative angular velocities is defined to acquire independent equations for relative velocities of turning pairs. Speed (teeth) ratio is used to express relative velocities of turning pairs as a function of input velocities. Finally, by using path and twist intensities matrices, link absolute angular velocities are determined in vectorial forms.

In T-T, on the other hand, the graph associated to the mechanism is presented in terms of labeling of links, joints and axes of rotation. According to the graph, paths are stated. By investigating the level of axes of rotation, transfer vertices (carrier

arms) are determined. By considering each link as a rigid body, terminal equations of turning and gear pairs are stated and for each terminal equation, gear ratio is obtained. Fundamental circuit equations are directly written from the graph and coaxial conditions are used for further kinematic analysis. Equations of output angular velocities in terms of input ones are developed in terms of gear ratios. Final results are obtained in vectorial forms by using Denavit-Hartenberg Convention.

Finally, results of the relative and absolute angular velocities in both methods are identical. Differences are just related to how kinematic analysis is performed, how the final results are obtained and which definitions and techniques are used in both methods. Benefits and drawbacks of both methods are also specified.

Keywords: Matroid Method, T-T Graph Method, Geared Robotic Mechanisms (GRMs), Kinematic analysis

ÖZ

Bu tez çalışması Matroid ve T-T Grafik metodlarının karşılaştırılmasını içermektedir. Grafik Metodu'na dayandırılmış yukarıda adı geçen grafik metodları dişli takımlarını de içeren mekanizmaların kinematik analizinde kullanılmaktadır. T-T grafik metodu yönsüz ve yönlü grafiklerin birleştirilmesiyle geliştirilmiştir. Buna zıt olarak, Matroid metodunda yönlü grafiklerden elde edilen çakışıklık matrisi kullanılmaktadır. Bu iki yöntemi kullanarak kinematik analiz uygulama amacıyla Dişli Robot Mekanizması (DRM) örnek bir mekanizma olarak nitelendirilmiştir.

Matroid metodunda, bağlantı ve birleşme nokta sayısına bağlı olarak kinematik zincirlere bağlı olan yönlü grafik üretilmektedir. Bu yönlü grafik için azaltılmış etkili devre uçlu, kapsayan ağaç, yol ve döngü kaynaklı matriksler üretilmiştir. Tüm dönüşlü ve dişli çiftler için göreceli açısal hız denklemleri tanımlanmıştır. Bağlantı noktalarının ve tabanın z-eksenlerinin arasındaki uzaklık açılarını bulmak amacıyla vidalama teorisi ve plücker kordinatları tanımlanmıştır. Dönüşlü ve birbiri içine geçmiş çiftler için 'Yoğun Dönüşlü Matriks' üretilmiştir. Göreceli açısal hız için dikgenlik koşulu tanımlanmış ve dönüşlü çiftlerin göreceli hızları için bağımsız denklemler elde edilmiştir. Dönüşlü çiftlerin göreceli hızlarını giriş hızı fonksiyonu olarak ifade etmek amacıyla hız (diş) oranı kullanılmıştır. Son olarak, yol ve döngü yoğunluklu matriksler ve bağlantı koşullu hız vektörel formlarda belirlenmiştir.

T-T metodunda ise mekanizmayla bağlantılı olan grafik bağlantıları, bağlantı noktaları ve devir eksenleri kapsamında sunulmuştur. Grafiğe göre yönler belirtilmiştir. Devir eksenlerinin düzeyini incelemekle, iletken köşe noktaları

(taşıyıcı kollar) belirlenmiştir. Her bir bağlantıyı sabit bir kısım olarak kabul etmekle, dönüşlü ve dişli çiftlerin nihai denklemleri belirtilmiş ve her nihai denklem için bir dişli oranı elde edilmiştir. Temel devre denklemleri doğrudan grafik aracılığıyla yazılmış ve eksendeş koşullar ek kinematik analiz için kullanulmıştır. Girişlerle ilgili açısal hız çıkışı denklemleri dişli oranları doğrultusunda üretilmiştir. Sonuçlar Denavit-Hartenberg kuralı kullanılarak vektörel form olarak elde edilmiştir.

Sonuç olarak, göreceli ve koşullu açısal hız sonuçları her iki yöntemde de aynı sonuçları vermiştir. Farklılıklar sadece kinematik analiz uygulama şeklinde, en son bulguların elde edilme yönteminde ve her iki yöntemde kullanılan tanımlamalar ve tekniklerde ortaya çıkmıştır. Her iki yöntemin yararları ve eksiklikleri ayrıca belirtilmiştir.

Anahtar Kelimeler: Matroid Metodu, T-T Grafik Methodu, Dişli Robot Mekanizmaları (DRM), Kinematik analiz

DEDICATION

This dissertation is dedicated to my lovely parents, SeyedAli & Vajiheh, and to my sister, Shokouh, for their love, devoting their time to support me. Further, I would like to dedicate this work to my beloved wife, Marzieh Rahmani Moghadam, for her encouragement and endless support.

ACKNOWLEDGMENTS

I would like to express my sincere thanks to Assoc. Prof. Dr. Mustafa Kemal Uyguroğlu for his continuous support and guidance in the preparation of this study. Without his invaluable supervision, all my efforts could have been short-sighted.

I owe a great debt of thanks to my parents, sister and specially my wife who supported me all throughout my studies. I would like to dedicate this study to them as an indication of their significance in this study as well as in my life.

Finally, a number of friends had always been around to support me morally. I would like to thank them as well.

TABLE OF CONTENTS

LIST OF TABLES

LIST OF FIGURES

LIST OF SYMBOLS/ABBREVIATIONS

$\mathbf{0}_{c,1}$	Zero-column matrix
$3D$	Three dimensional
$\mathbf{A}_{c,t}$	Position matrix in terms of tooth ratio
a	Joint offset length
B	Co-tree
$\mathbf{C}$	Cycle basis matrix
C	Cycle space
c	Number of gear (meshing) pairs/number of dash edges/number of chords/number of fundamental cycles
D	Matroid digraph
$\mathbf{D}_{0,k}$	Orthogonal direction-cosine matrix
d	Translational displacement
d_i	Pitch diameter of gear i
d_j	Pitch diameter of gear j
E	Set of edges/degree of freedom (input velocities)
e	A chord from co-tree
$\mathbf{G}$	Matrix associated with arcs
$\mathbf{G}^*$	Matrix associated with chords
$\mathbf{I}^0_{c,k}$	Distance vector between c and k
$\widehat{\mathbf{I}}^0_{c,k}$	Skew symmetric of $\mathbf{I}^0_{c,k}$
i	Input link (vertex)
i_c	Tooth ratio

j	Output link (vertex)
k	Number of joints/number of directed edges/carrier arm (transfer vertex)
$(i, j)(k)$	The gear pair and its carrier arm
L_k	x-component of $\mathbf{u}_k^0$
M1, *M2*, and *M3*	Input actuators
M_k	y-component of $\mathbf{u}_k^0$
N	Set of nodes
N_i	Number of teeth of gear *i*
N_j	Number of teeth of gear *j*
N_k	z-component of $\mathbf{u}_k^0$
N_{ji} / N_{ij}	Gear ratio
n	Number of links and number of nodes
n_{tail}	Starting node of a directed edge
n_{head}	End node of a directed edge
$P_{c,k}$	x-component of $\mathbf{r}_{c,k}^0$
$\mathbf{P}_{c,t}$	Position matrix
${}^{i-1}\mathbf{P}_i$	General homogenous position sub-matrix
$Q_{c,k}$	y-component of $\mathbf{r}_{c,k}^0$
$R_{c,k}$	z-component of $\mathbf{r}_{c,k}^0$
${}^{i-1}\mathbf{R}_i$	General homogenous orientation sub-matrix
r	Rank of cucle-basis matrix/number of outputs (unknown variables)
$\mathbf{r}_{c,k}^0$	position vector of z_k
$\hat{\mathbf{s}}_k^0$	Twist matrix

$\mathbf{T}$	Spanning tree matrix
${}^{i-1}\mathbf{T}_i$	General homogenous transformation matrix
T	Spanning tree
^{T}	transpose operation
t	Number of turning pairs and number of continuous edges
$\mathbf{U}$	Identity matrix
$\mathbf{u}$	Unit vector w.r.t. local z-axis
$\mathbf{u}_k^0$	Unit vector w.r.t. base z-axis
$\hat{\mathbf{u}}_{c,k}^0$	Screw matrix (dual vector)
x_k	x-axis of relative motion (local frame)
y_k	y-axis of relative motion (local frame)
$\mathbf{Z}$	Path matrix
z_k	z-axis of relative motion (local frame)
$z_{t,n}$	Entry of path matrix
α	Joint twist angle
$\mathbf{\Gamma}$	Reduced incidence node-edge matrix
θ	Joint angle
$\dot{\theta}_k$	Angular velocity variable
$\dot{\boldsymbol{\theta}}_{k,1}$	Twist intensities matrix
φ_k	offset angles between z-axis of base and z-axes of turning axes
$\bar{\boldsymbol{\omega}}_{ji}$	Vectorial form of angular velocity of link *j* w.r.t. link *i*
ω_{ji}	Angular velocity of link *j* w.r.t. link *i*
ω'_{ik}	Angular velocity of link *i* w.r.t. carrier arm *k*
ω'_{jk}	Angular velocity of link *j* w.r.t. carrier arm *k*
$\boldsymbol{\omega}_n^0$	Absolute velocity matrix

Chapter 1

INTRODUCTION

1.1 Introduction

In recent decades, a number of methods and approaches i.e. either analytical or graphical have been released for kinematic analysis of mechanisms including gear systems. One of the widely used analytical methods for this kind of analysis is the Willis inversion method of motion [1]. Tabular methods [2-4] which are generated according to Willis' inversion method are easier to some extent. Vector-loop methods [5, 6] and matrix methods [7-9] can be also considered as examples of other analytical methods.

On the other hand, a number of various graphical methods have been developed for modeling of the geared mechanisms such as Signal Flow Graphs [10], Bond Graphs [11-13], and Linear Graph representation [14-24]. Linear Graph model is widely used as graph representation of geared systems such that links and joints are modeled by vertices and edges respectively. Modeling based on graph representation is performed for analysis and synthesis of gear trains. The analysis might be either kinematic or dynamic or both of them and the synthesis is to create design models of gear trains. These methods are useful for analyzing a mechanism (gear train) with large number of links and joints as well as applying in computer algorithms. Indeed, graph-based methods can be efficiently considered as computer and Artificial Intelligent (AI) aided approaches for modeling of mechanisms [25-31]. By using

graph-based approaches, comparison of the results of kinematical analysis can be done within stages of design. Gear mechanism's atlases of design can be completely created by graphical methods [32] which cannot be prepared by using other approaches.

Some of the above mentioned methods (e.g. Willis inversion method of motion and Tabular methods), in general, focus on input and output displacement and velocity whereas the motions of the planet gears are not perceived. What's more, these methods have a lack of generality and they are just applicable to the gear trains which consist of links with parallel axes of rotation i.e. Epicyclic Gear Trains (EGTs). Therefore, such gear trains which consist of links with non-parallel axes of rotation i.e. Bevel Gear Trains (BGTs) cannot be analyzed by these methods and kinematic analysis of these gear trains were excluded [6, 22] due to the complexity of the three-dimensional motion of links. This motion is generated by two independent rotations about two intersected axes plus a rotation of end-effector about its axis. BGTs [33-40] are included in Geared Robotics Mechanisms (GRMs) [41] in order to acquire any arbitrary orientation of the end-effector as well as increase the flexibility of the structure by generating non-parallel axes of rotation.

Matroid Theory [42, 43] is one of the theoretical aspects in combinatorics which is a branch of pure mathematics and it was released by Hassler Whitney [44]. In this theory, linear algebra and graph theory are combined to generalize linear independence in vector space. Matroid was applied to study of electrical and mechanical systems [45]. By using the application of this theory, Talpasanu *et al.* [46-49] introduced Matroid method to kinematic and dynamic analysis of mechanical systems.

T-T Graph method is published by Uyguroğlu *et al.* [50, 51] to overcome weaknesses of non-oriented [15, 22, 35] and oriented graphs [52-54]. In this method, non-oriented and oriented graphs are combined to analysis of geared mechanical systems. In fact, by inserting the advantage of non-oriented graph technique which is to find the carrier arm (transfer vertex) to the oriented graph technique, T-T graph method was proposed. In the oriented graph method, arrows are used to indicate the terminal ports between nodes as well as direction of a pair of meters for measuring a pair of complementary terminal variables [52]. A pair of complementary terminal variables is essential to represent the physical behavior of the mechanism [54]. The complementary terminal variables are terminal *across* and terminal *through* variables [52]. In mechanical systems, translational and rotational velocities are considered as the terminal across variables and forces and moments are considered as the terminal through variables.

1.2 Thesis Overview

This thesis is partitioned in four chapters:

- Chapter 1: by reviewing literature of previous works states some analytical and graphical methods which are used in kinematic analysis of geared systems. Then, it mentions about BGTs and GRMs and their benefits. Finally, it reviews previous works on T-T Graph and Matroid methods, which will be compared.
- Chapter 2: the fundamentals and definitions of both methods will be defined in this chapter as well as how it can be possible to model a geared mechanism by using these methods.
- Chapter 3: in this chapter, first, the sample geared mechanism will be illustrated and all links and joints will be defined. Then, kinematic analysis of this mechanism will be done by applying two methods to it.

- Chapter 4: consists of comparison of results of both methods in addition to future works.

1.3 Thesis Objectives

In this thesis by considering a geared system with large number of links and joints first the kinematic analysis of this mechanism will be done by T-T Graph and Matroid methods and then results of these methods will be compared with each other. Besides, as will be explained and seen, Screw Theory and Denavit-Hartenberg Convention will be applied to Matroid and T-T respectively because of obtaining output velocities in vectorial forms thus these results also will be compared. Finally, the advantages and disadvantages of both T-T Graph and Matroid will be outlined.

Chapter 2

GRAPH AND METHODS

2.1 Introduction

It is worthwhile to describe a mechanism as a linear graph in which links and kinematic pairs correspond to vertices and edges respectively. Labeling of edges is performed according to the type of pairing i.e. turning- or gear-pairs. In following sections, fundamental parts of both methods will be discussed and then in chapter 3 (Mechanism and Kinematic Analysis) both methods will be applied to the desired mechanism and the final results will be obtained.

In Section 2.2 of this chapter, Matroid method was expressed then T-T graph method will be expressed in Section 2.3. Both methods use the fundamental definitions of Graph Theory [47, 50]. However, Matroid Method uses Algebra and Matroid Theory beside this [49]. There exist some definitions which are applicable in both methods so first we define all of them in Matroid method and in T-T Graph method wherever they are needed we will refer to Matroid part.

In addition, in both methods for defining all the final results as the vectorial quantities and distinguishing special cases we must use other theories as well, since graph-theoretic approaches give generic information. In fact, in Matroid method the initial steps are just some fundamentals definitions which are developed according to Graph and Algebra. So, for kinematic analysis Plücker coordinates and Screw theory

[55] is applied as a method to obtain final result. In T-T Graph method, although the kinematic analysis is performed in initial steps, the results are not in the vectorial form (the scalar of the results is obtained). Hence, the Denavit-Hartenberg Convention [56] will be used in this method to define the results in the vectorial form [51, 54].

2.2 Matroid Method

2.2.1 Labeling Links and Joints

In each mechanical structure, there are *n* number of links and *k* number of joints. For labeling [47], following steps are considered:

I. Functional schematic:

a) Start from ground link (reference link) and 0 is assigned to this link.

b) For other links i.e. gears and transform arms (carriers), we use 1, 2,…, *n* as labels.

c) For labeling joints, we label $k = t + c$ pairs (*t* is the number of turning pairs and *c* is the number of gear pairs). $n+1,..., n+t$ labels are considered for turning pairs and $n+1+t,...,n+k$ labels are considered for gear pairs.

II. Digraph:

a) Reference link is dedicated by node 0.

b) Other links are illustrated by labeled nodes from 1, 2,…, *n*.

c) Solid arrows are used to show turning pair joints.

d) Dash lines are used to express gear pair joints.

These steps will be applied on sample mechanism in Section 3.2.1 and associated digraph will be shown in Figure 3.2.

For each structure, there exists a digraph, defined *N* = (*D*, *E*), which has a collection of $n+1$ nodes (one node for reference link and *n* nodes for links). This collection is

illustrated as $N(D) = \{0, 1, 2, \ldots, n\}$. These nodes are connected by k directed edges, $E(D) = \{n+1, ..., n+t, n+1+t, ..., n+k\}$ [42, 47]. Turning pairs are represented by t directed edges and gear pairs are represented by c directed dash edges, $k = t + c$. Each set [*tail,head*] of nodes is assigned to a k directed edge which is an oriented arrow from n_{tail} to n_{head}, for instance in Figure 3.2, edge 10 assigns to set [0,1].

According to fundamental definitions of Matroid theory, in mechanisms with the large number of links (nodes) and joints (edges), there exist some rules to find independent cycles. Although in sample mechanism, Figure 3.1, matroid theory is used, application of this theory is discussed rather than pure theoretical aspects. Therefore, by avoiding to pass the theory of Matroid, for finding independent cycle set, it will be sufficient to refer to Section 2.2.2.

2.2.2 Path, Spanning Tree and Fundamental Cycles

A sequence of nodes and edges where all nodes are different is defined as a Path. The path is called Cycle (circuit) if the last node coincides with the first one (each cycle is started from dash edge). In digraph *D*, by cutting the edges related to *c* gear pairs one could obtain spanning tree i.e. every node lies in the tree without any circuits (cycles). Edges of the digraph are divided into two sets, Tree (*T*) and Co-tree (*B*). *E(T)* and *E(B)* sets contain arcs (turning pairs' edges which belong to spanning tree) which are labeled from $n+1$ to $n+k-c$ and chords (gear pairs' edges which do not belong to spanning tree) which are labeled from $n+k-c+1$ to $n+k$ respectively [22, 23].

Since the edges are partitioned into arcs and chords (solid and dash lines respectively in Figure 3.2) and if *e* is one of the chords from Co-tree set then $T \cup \{e\}$ contains a

Fundamental Cycle (circuit). Adding each chord from Co-tree to Spanning tree separately will form the basis, *C*, for cycle space. So, other combination and possibilities of circuits will be linearly dependent to this basis. For each mechanism with *n* nodes and *k* edges (the spanning tree which is made up of arcs will have *n* nodes and $n-1$ edges) there will be *c* chords (gear pairs) as well as *c* fundamental cycles according to Euler's formula [46]:

$$c = k - n \tag{2.1}$$

2.2.3 Incidence Node-Edge Matrix

In the oriented graph, the Incidence Node-Edge matrix $\mathbf{\Gamma}^0$ is a $(n+1)\times k$ matrix. For each edge *k* there will be $-1, 0, \text{and} +1$ entries [23]. If edge enters node, the entry will be $+1$, it will be -1 if edge leaves node and otherwise it will be zero. In other words, each column will have just two entries related to two nodes which are connected with each other by respective edge and summation of entries is always equal to zero in each column. Columns and rows in Incidence matrix indicate joints and links respectively. It can be observed that in Incidence matrix rows are dependent. That is, by deleting the first row other rows will be independent. The first row can be acquired in terms of other rows' entries. It means, in each column if there is $-1 \text{and} +1$, the entry of first row in that column will be zero. It will be $-1 \text{or} +1$ if in related column there is $+1 \text{or} -1$ respectively.

2.2.4 Reduced Incidence Node-Edge Matrix

Deleting the row which is related to the ground link (link 0) from incident matrix $\mathbf{\Gamma}$ will be result in the Reduced Incidence Node-Edge matrix. This matrix is divided into two sub-matrices because $k = t + c$ and $t = n$:

$$\mathbf{\Gamma} = \left[\mathbf{G} \,\vdots\, \mathbf{G}^*\right] \tag{2.2}$$

where $\mathbf{G}$ is an $n \times n$ matrix, which is associated with the arcs, and its columns are

labeled as the turning pairs (edges related to spanning tree) and an $n \times c$ matrix $\mathbf{G}^*$, which is associated with the chords, and its columns are labeled as the gear pairs (edges related to co-tree) of the mechanism.

2.2.5 Path Matrix

Path matrix $\mathbf{Z}$ [49] is a $t \times n$ matrix and because $t = n$ so it is a square matrix. This matrix comes from the spanning tree, where turning pair *t* and link *n* is presented in each row (the edge of spanning tree) and each column (the node of spanning tree) respectively. Here, again, $z_{t,n}$ can be $-1, 0, \text{and} +1$. Spanning tree consists of paths which are made up of edges related to turning pairs. As a result, if edge *t* belongs to one of these paths which are started from node *n* toward the ground link and its orientation is the same as path's direction, $z_{t,n}$ becomes +1. If it belongs to the path but the orientation is opposite, $z_{t,n}$ becomes -1. $z_{t,n} = 0$ if edge does not belong to the related path. The path matrix will be used for determining the link absolute angular velocities. There exist following relations which are important for the kinematic analysis of the mechanism [46]:

$$\mathbf{ZG} = \mathbf{GZ} = -\mathbf{U} \qquad \text{and} \qquad \mathbf{Z}^T\mathbf{G}^T = \mathbf{G}^T\mathbf{Z}^T = -\mathbf{U} \tag{2.3}$$

2.2.6 Spanning Tree Matrix and Cycle Basis Matrix

The Spanning Tree matrix [23, 47] is denoted by $\mathbf{T}_{c \times t}$, each fundamental cycle has its own row and the *t* turning pairs are considered as the columns. This matrix is obtained by product of $\mathbf{G}^*$ and path matrix:

$$\mathbf{T} = \mathbf{G}^{*T} \cdot \mathbf{Z}^T \tag{2.4}$$

$\mathbf{C}_{c \times k}$ is the Cycle Basis matrix, each fundamental cycle and each directed edge are denoted in corresponding row and column respectively. As $k = t + c$, this matrix

has two sub-matrices: $\mathbf{T}_{c\times t}$ with the turning pairs (arcs) as columns' labels (tree's edges) and unit matrix $\mathbf{U}_{c\times c}$ with the gear pairs (chords) as columns' labels (co-tree's edges):

$$\mathbf{C} = \left[\mathbf{T} \,\vdots\, \mathbf{U}\right] \tag{2.5}$$

In each row of $\mathbf{C}$, non-zero components indicate the edges which belong to the corresponding cycle. These elements can be positive, negative, and zero. +1 entries are related to the edges which have the same orientation as the cycle direction (in each fundamental cycle, cycle direction is determined according to the orientation of chord which exists in that cycle). Edges which their orientation is opposite of the cycle direction will have -1 entries. 0 entries are for those edges which do not belong to the cycle.

2.3 T-T Graph Method

2.3.1 Labeling Links, Joints, and Axes of Rotation

By using the following steps the labeling of a mechanism with *n* number of links and *k* number of joints will be done in T-T Graph method [50]:

I. Functional schematic:

1) Ground link is numbered by 0.

2) Links are numbered from 1 to *n*.

3) *a, b, c,...* are considered as labels of the turning pairs' axes.

II. Digraph:

1) Vertex 0 refers to reference base.

2) Each link is represented by corresponding numbered vertex.

3) Turning pair is labeled by ω_{ji} and the label of axis location are indicated by oriented heavy edge. This edge orients from output vertex (link) *j* to input one *i* as

shown in Figure 2.1.

4) Gear mesh and corresponding carrier arm is labeled by ω'_{ik} and ω'_{jk} and represented by oriented light edge which orients from vertices *i* and *j* to transfer vertex (carrier arm) *k* as shown in Figure 2.1.

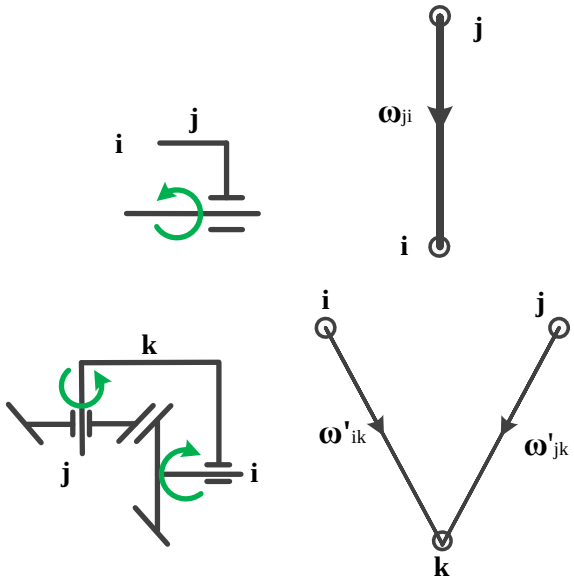

Figure 2.1: The representation of turning and gear pairs.

The labeling steps of T-T Graph method will be applied on sample mechanism in Section 3.3.1 and associated digraph will be shown in Figure 3.5.

2.3.2 Fundamental Circuits and Transfer Vertices

In this method, directed heavy lines which represent the turning pairs make a tree (spanning tree) and called tree branches while directed light line which indicate the gear pairs constitute a complementary tree (co-tree) and called chords [52] (geared edges). In fact, a unique spanning tree will be acquired by deleting all chords from the graph. Therefore, by adding the chords one by one to the spanning tree fundamental circuits will be obtained. In other words, each fundamental circuit (f-circuit) contains one chord (gear pair or meshing joint) so the number of f-circuits is

equal to the number of chords (gear pairs or meshing joints). In spanning tree a sequence of vertices which are connected by edges is called a path such that all vertices must be different (refer to Section 2.2.2 for more details).

Determination of transfer vertex (carrier arm) in this method [50] is so important in order to obtain the terminal equations and make the procedure of analysis faster than Matroid. For doing this, after labeling the axes of turning pairs, by moving on each path of the spanning tree and go from starting vertex to the end vertex through branches, the transfer vertex will be determined. Indeed, a vertex is called transfer vertex such that the level of edges of one side is different from the level of edges of other side. Note that, there must exist a transfer vertex in each f-circuit. $(i, j)(k)$ indicates a gear pair and its carrier arm where *i* and *j* are the vertices of the gear pair and *k* is the transfer vertex.

2.3.3 Terminal Equations and Coaxial Conditions

For kinematic analysis of any gear train (included bevel gear) the terminal equations can be utilized [52, 54]. As explained above, let set $(i, j)(k)$ be the gear pair and its carrier arm then the terminal equation can be derived as follows:

$$(i, j)(k): \omega_{ik} = \pm N_{ji}\,\omega_{jk} \tag{2.6}$$

where ω_{ik} and ω_{jk} represent the angular velocities of gears *i* and *j* respectively w.r.t the carrier arm *k* and N_{ji} is the gear ratio between those gears:

$$N_{ji} = \frac{N_j}{N_i}\left(= \frac{d_j}{d_i}\right) \tag{2.7}$$

where $N_j\,(d_j)$ and $N_i\,(d_i)$ are the number of teeth (or pitch diameter) of gears *j* and *i*. This ratio will be positive or negative according to the right-hand-screw rule. That

is, this ratio will be negative if clock-wise rotation of input gear *i* w.r.t carrier arm yields a counter clock-wise rotation of output gear *j* and it will be positive if clock-wise rotation of input gear *i* w.r.t carrier arm yields a clock-wise rotation of output gear *j*. Following relations are defined for all gears *i* and *j*:

$$\omega_{ij} = -\omega_{ji} \quad \text{and} \quad N_{ij} = \frac{1}{N_{ji}} \tag{2.8}$$

The coaxial condition [35] is used for further kinematic analysis. Consider *p*, *q*, and *r* as three coaxial links then by following condition the relative angular velocities amongst these links can be obtained:

$$\omega_{pq} = \omega_{pr} - \omega_{qr} \tag{2.9}$$

where ω_{pq} denotes the angular velocity of link *p* w.r.t link *q*.

Chapter 3

MECHANISM AND KINEMATIC ANALYSIS

3.1 The Mechanism

In this chapter, Geared Robotic Mechanism (GRM) is considered as an example. GRMs are closed-loop configurations which are used to reduce the mass and inertia of the actuators' loads. Gear trains in GRMs are employed such that actuators can be placed as closely as possible to the base. Figure 3.1 shows functional schematic of desired GRM. It is a 3-DOF (Degree of Freedom) mechanism which has the same movement as arm and wrist. It is observed that links and joints (gear train) are used to transmit the rotation of the inputs to the end effector. The motion of end effector is produced by links 4, 5, and 6 as inputs. The end effector is attached to link 3 and carried by link 2. The rotation of link 3 is caused by *M3* through 6 and 7 links and the rotation of links 1 and 2 is made by *M1* through link 4 and *M2* through link 5 respectively.

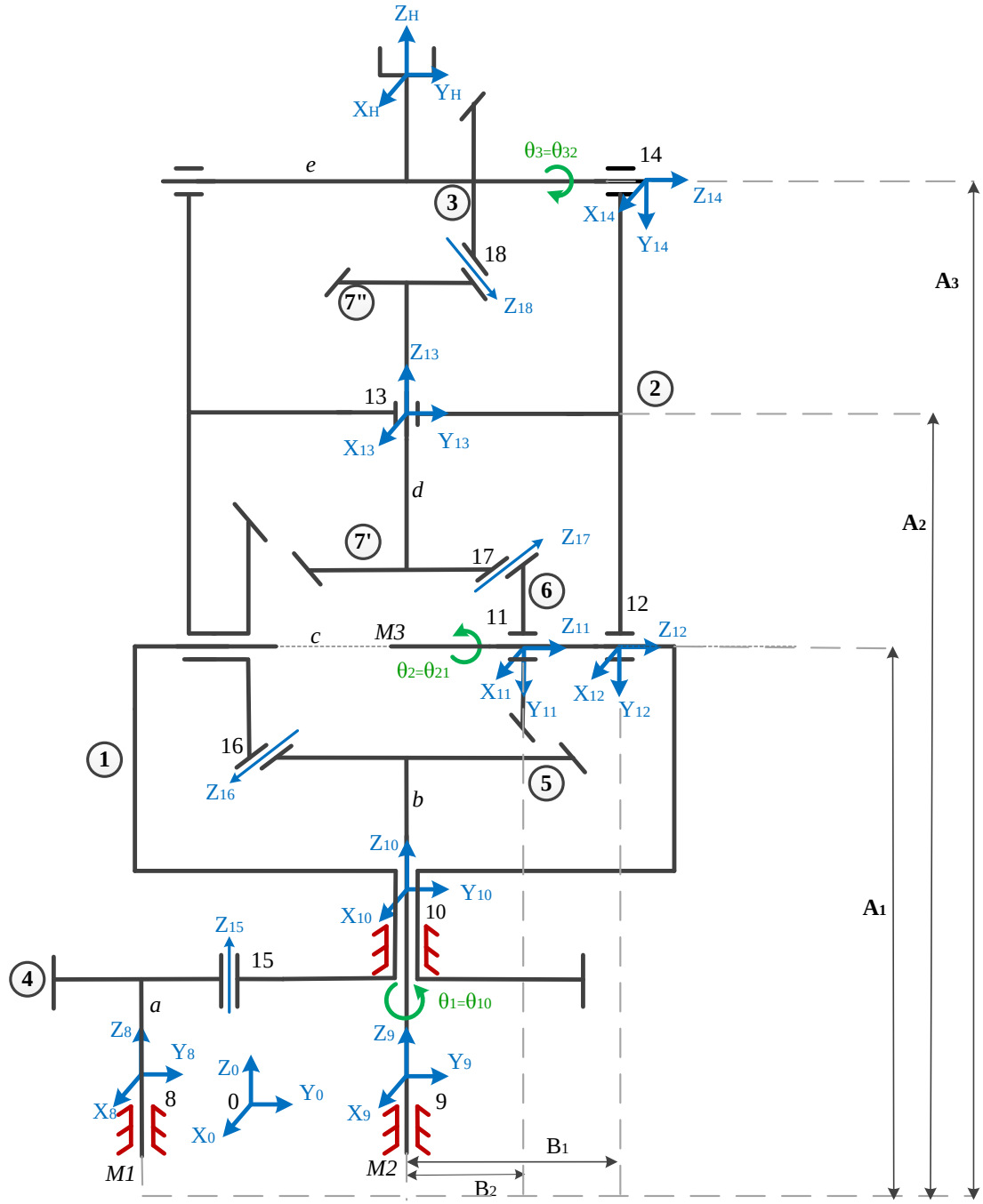

Figure 3.1: The GRM mechanism.

3.2 Kinematic Analysis using Matroid Method

3.2.1 Matroid Digraph and Corresponding Matrices

The mechanism in Figure 3.1 consists of $n = 7$ links and $k = 11$ joints which the connections between links are supplied by turning and meshing joints. The following

labeling which is assigned to links and joints of sample mechanism is used in Matroid method:

- 0 is assigned to ground link.
- 1, 2, 3, 4, 5, 6, and 7 are assigned to gears and carriers.
- 8, 9, 10, 11, 12, 13, 14, 15, 16, 17, and 18 are assigned to joints.

In this mechanism 4, 5, and 6 are sun gears (input links), 1 and 2 are carriers and $3, 7', \text{and} 7''$ are planet gears. There exist joints such that 8, 9, 10, 11, 12, 13, and 14 are turning pairs' labels ($t = 7$) and 15, 16, 17, and 18 are gear pairs' labels ($c = 4$). The labeling of this mechanism which is used in Matroid method is illustrated in the Figure 3.2:

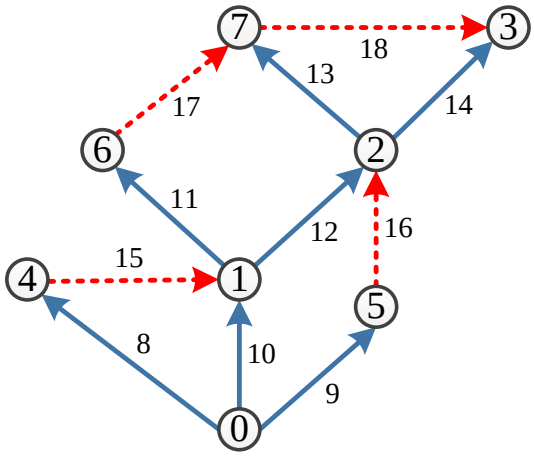

Figure 3.2: Mechanism associated digraph.

There is the corresponding digraph to mechanism in Figure 3.2. $N(D) = \{0,1,2,3,4,5,6,7\}$ is the set of nodes of this digraph with 7 nodes (1, 2, 3, 4, 5, 6, and 7) attached to the $n = 7$ mobile links and one node (0) attached to the ground. These nodes are connected to each other by $k = 11$ directed edges which 8, 9, 10, 11, 12, 13, and 14, $t = 7$, are related to turning pairs and 15, 16, 17, and 18, $c = 4$, correspond to gear pairs.

The pair set of $E(D)=\{[0,1],[0,4],[0,5],[1,2],[1,6],[2,3],[2,7],[1,4],[5,2],[6,7],[7,3]\}$ is assigned to the set of directed edges $E(D)=\{8,9,10,11,12,13,14,15,16,17,18\}$. In order to interpret relative angular velocities between links easily, each edge is oriented from its lower-level node to higher-level one. In other words, it is better that all edges connected to node 0 are oriented away from this node (8, 9, and 10 are away from node 0) and edges which are assigned to carriers and planets oriented toward the nodes (e.g. 13 and 14 are oriented toward 7 and 3 respectively) though it is possible for the directed edges to orient arbitrarily.

The spanning tree of sample mechanism which was defined in Section 2.2.2 is illustrated in Figure 3.3 corresponding to Figure 3.2.

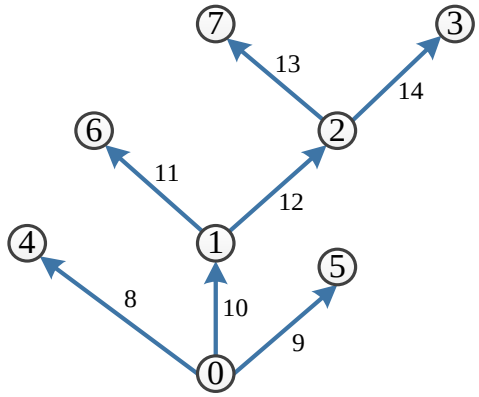

Figure 3.3: Spanning tree of the digraph

For sample mechanism and its digraph, the spanning tree has $N(T)=\{0,1,2,3,4,5,6,7\}$ and $E(T)=\{8,9,10,11,12,13,14\}$ sets and the co-tree has $E(B)=E(D)-E(T)=\{15,16,17,18\}$ set. There exist fundamental cycle set $C(D)=\{C_{15},C_{16},C_{17},C_{18}\}$ which has $c=4$ cycles corresponding to meshing (transfer) joints. Fundamental cycles of desired mechanism are shown in Figure 3.4. That is, $C_{15}=\{15,8,10\}, C_{16}=\{16,12,10,9\}$, $C_{17}=\{17,13,12,11\}$, $C_{18}=\{18,14,13\}$.

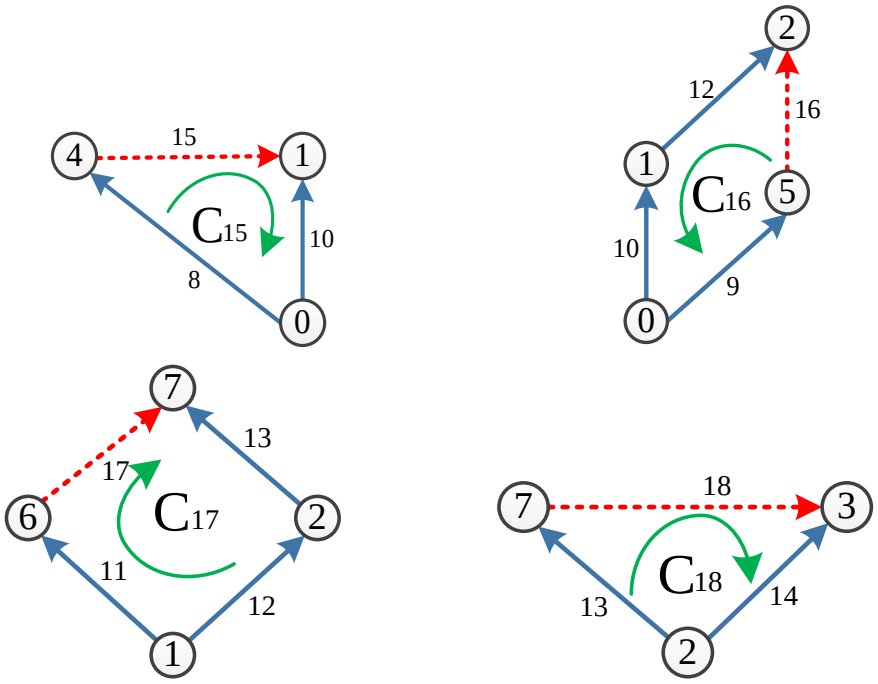

Figure 3.4: Fundamental cycles

In the following the matrices which are defined in the Section 2.2 are acquired and after that the procedure of Matroid method and the kinematic analysis of desired mechanism using this method will be shown.

For the digraph in Figure 3.2 the Incidence Node-Edge Matrix and the Reduced Incidence Node-Edge Matrix are:

$$\mathbf{\Gamma}^0 = \begin{array}{c} \\ 0\rightarrow \\ 1\rightarrow \\ 2\rightarrow \\ 3\rightarrow \\ 4\rightarrow \\ 5\rightarrow \\ 6\rightarrow \\ 7\rightarrow \end{array} \begin{array}{c} \begin{array}{ccccccccccc} 8 & 9 & 10 & 11 & 12 & 13 & 14 & 15 & 16 & 17 & 18 \\ \downarrow & \downarrow & \downarrow & \downarrow & \downarrow & \downarrow & \downarrow & \downarrow & \downarrow & \downarrow & \downarrow \end{array} \\ \left[\begin{array}{ccccccccccc} -1 & -1 & -1 & 0 & 0 & 0 & 0 & 0 & 0 & 0 & 0 \\ \hline 0 & 0 & 1 & -1 & -1 & 0 & 0 & 1 & 0 & 0 & 0 \\ 0 & 0 & 0 & 0 & 1 & -1 & -1 & 0 & 1 & 0 & 0 \\ 0 & 0 & 0 & 0 & 0 & 0 & 1 & 0 & 0 & 0 & 1 \\ 1 & 0 & 0 & 0 & 0 & 0 & 0 & -1 & 0 & 0 & 0 \\ 0 & 1 & 0 & 0 & 0 & 0 & 0 & 0 & -1 & 0 & 0 \\ 0 & 0 & 0 & 1 & 0 & 0 & 0 & 0 & 0 & -1 & 0 \\ 0 & 0 & 0 & 0 & 0 & 1 & 0 & 0 & 0 & 1 & -1 \end{array}\right] \end{array} \tag{3.1}$$

$$\mathbf{\Gamma} = \left[\begin{array}{ccccccc:cccc} 0 & 0 & 1 & -1 & -1 & 0 & 0 & 1 & 0 & 0 & 0 \\ 0 & 0 & 0 & 0 & 1 & -1 & -1 & 0 & 1 & 0 & 0 \\ 0 & 0 & 0 & 0 & 0 & 0 & 1 & 0 & 0 & 0 & 1 \\ 1 & 0 & 0 & 0 & 0 & 0 & 0 & -1 & 0 & 0 & 0 \\ 0 & 1 & 0 & 0 & 0 & 0 & 0 & 0 & -1 & 0 & 0 \\ 0 & 0 & 0 & 1 & 0 & 0 & 0 & 0 & 0 & -1 & 0 \\ 0 & 0 & 0 & 0 & 0 & 1 & 0 & 0 & 0 & 1 & -1 \end{array}\right] \tag{3.2}$$

The Path Matrix for the spanning tree in Figure 3.3 is:

$$\mathbf{Z} = \begin{array}{c} \begin{array}{ccccccc} 1 & 2 & 3 & 4 & 5 & 6 & 7 \\ \downarrow & \downarrow & \downarrow & \downarrow & \downarrow & \downarrow & \downarrow \end{array} \\ \left[\begin{array}{ccccccc} 0 & 0 & 0 & -1 & 0 & 0 & 0 \\ 0 & 0 & 0 & 0 & -1 & 0 & 0 \\ -1 & -1 & -1 & 0 & 0 & -1 & -1 \\ 0 & 0 & 0 & 0 & 0 & -1 & 0 \\ 0 & -1 & -1 & 0 & 0 & 0 & -1 \\ 0 & 0 & 0 & 0 & 0 & 0 & -1 \\ 0 & 0 & -1 & 0 & 0 & 0 & 0 \end{array}\right] \end{array} \begin{array}{l} 8 \rightarrow \\ 9 \rightarrow \\ 10 \rightarrow \\ 11 \rightarrow \\ 12 \rightarrow \\ 13 \rightarrow \\ 14 \rightarrow \end{array} \tag{3.3}$$

Finally, the Spanning Tree and the Cycle Basis Matrices of sample mechanism are:

$$\mathbf{T} = \begin{array}{c} \begin{array}{ccccccc} 8 & 9 & 10 & 11 & 12 & 13 & 14 \\ \downarrow & \downarrow & \downarrow & \downarrow & \downarrow & \downarrow & \downarrow \end{array} \\ \left[\begin{array}{ccccccc} 1 & 0 & -1 & 0 & 0 & 0 & 0 \\ 0 & 1 & -1 & 0 & -1 & 0 & 0 \\ 0 & 0 & 0 & 1 & -1 & -1 & 0 \\ 0 & 0 & 0 & 0 & 0 & 1 & -1 \end{array}\right] \end{array} \begin{array}{l} C_{15} \rightarrow \\ C_{16} \rightarrow \\ C_{17} \rightarrow \\ C_{18} \rightarrow \end{array} \tag{3.4}$$

$$\mathbf{C} = \begin{array}{c} \begin{array}{ccccccc:cccc} 8 & 9 & 10 & 11 & 12 & 13 & 14 & 15 & 16 & 17 & 18 \\ \downarrow & \downarrow & \downarrow & \downarrow & \downarrow & \downarrow & \downarrow & \downarrow & \downarrow & \downarrow & \downarrow \end{array} \\ \left[\begin{array}{ccccccc:cccc} 1 & 0 & -1 & 0 & 0 & 0 & 0 & 1 & 0 & 0 & 0 \\ 0 & 1 & -1 & 0 & -1 & 0 & 0 & 0 & 1 & 0 & 0 \\ 0 & 0 & 0 & 1 & -1 & -1 & 0 & 0 & 0 & 1 & 0 \\ 0 & 0 & 0 & 0 & 0 & 1 & -1 & 0 & 0 & 0 & 1 \end{array}\right] \end{array} \begin{array}{l} C_{15} \rightarrow \\ C_{16} \rightarrow \\ C_{17} \rightarrow \\ C_{18} \rightarrow \end{array} \tag{3.5}$$

3.2.2 Screw Theory and Equations for Relative Angular Velocities of Turning Pairs

Screw matrix [55] (dual vector) $\hat{\mathbf{u}}_{c,k}^{0}$ defines spatial displacement which is a combination of rotation about a line and translation along the same line. Indeed, z_k axis of relative motion will be considered as the line which will define the geometry of each axis. This is a six-dimensional (6×1 column matrix) vector which is constructed by a pair of 3*D* vectors i.e. linear velocity and angular velocity.

$$\hat{\mathbf{u}}_{c,k}^{0} = \begin{pmatrix} \mathbf{u}_k^0 \\ \mathbf{r}_{c,k}^0 \end{pmatrix} = \begin{pmatrix} L_k & M_k & N_k \vdots P_{c,k} & Q_{c,k} & R_{c,k} \end{pmatrix}^T \tag{3.6}$$

Along each pair, the local frame (x_k, y_k, z_k) is selected in terms of the orientation of z_k and they have unit vector $\mathbf{u} = \begin{pmatrix} 0 & 0 & 1 \end{pmatrix}^T$ with respect to their local z-axis and unit vector $\mathbf{u}_k^0 = \begin{pmatrix} L_k & M_k & N_k \end{pmatrix}^T$ w.r.t base z-axis (reference frame). The orientation of each z_k (first vector in screw) can be obtained as follows:

$$\mathbf{u}_k^0 = \mathbf{D}_{0,k} \cdot \mathbf{u} \tag{3.7}$$

where $\mathbf{D}_{0,k}$ is transformation Matrix (orthogonal direction-cosine matrix):

$$\mathbf{D}_{0,k} = \begin{bmatrix} \cos\varphi_{x_0,x_k} & \cos\varphi_{x_0,y_k} & \cos\varphi_{x_0,z_k} \\ \cos\varphi_{y_0,x_k} & \cos\varphi_{y_0,y_k} & \cos\varphi_{y_0,z_k} \\ \cos\varphi_{z_0,x_k} & \cos\varphi_{z_0,y_k} & \cos\varphi_{z_0,z_k} \end{bmatrix} \tag{3.8}$$

After finding all angles between coordinates, $\mathbf{D}_{0,k}$ can be defined as a pure rotational matrix about x-axes:

$$\mathbf{D}_{0,k} = \begin{bmatrix} 1 & 0 & 0 \\ 0 & \cos\varphi_k & -\sin\varphi_k \\ 0 & \sin\varphi_k & \cos\varphi_k \end{bmatrix} \tag{3.9}$$

where φ_k are offset angles between z-axis of base and z-axes of turning axes.

Since unit vectors w.r.t local z-axis (local frame) have the form:

$$\mathbf{u} = \begin{pmatrix} 0 & 0 & 1 \end{pmatrix}^T \tag{3.10}$$

Then from Eq. (3.9) unit vectors w.r.t base z-axis (reference frame) will have the form:

$$\mathbf{u}_k^0 = \begin{pmatrix} L_k & M_k & N_k \end{pmatrix}^T \tag{3.11}$$

where $L_k = 0; M_k = -\sin\varphi_k; N_k = \cos\varphi_k$ since the $\mathbf{u}$ vector just has *z* component so just third column of $\mathbf{D}_{0,k}$ matrix is valid for $\mathbf{u}_k^0$ vector.

$\mathbf{r}_{c,k}^0$ is the position vector of z_k (second vector in screw) and can be acquired as below:

$$\mathbf{r}_{c,k}^0 = \mathbf{I}_{c,k}^0 \times \mathbf{u}_k^0 \tag{3.12}$$

The distance vectors $\mathbf{I}_{c,k}^0$ (a lower index shows that $\mathbf{I}$ has orientation from *c* to *k* and upper one indicates that this orientation is w.r.t. base) can be calculated by Eq (3.13):

$$\mathbf{I}_{c,k}^0 = \begin{pmatrix} x_{c,k} \\ y_{c,k} \\ z_{c,k} \end{pmatrix} = \begin{pmatrix} x_k \\ y_k \\ z_k \end{pmatrix} - \begin{pmatrix} x_c \\ y_c \\ z_c \end{pmatrix} \tag{3.13}$$

where $x_{c,k} = 0$ since all rotations are done about x-axis so there does not exist any displacement along this axis.

Then from Eq. (3.12) and (3.13), one can conclude that:

$$\mathbf{r}_{c,k}^0 = \begin{pmatrix} P_{c,k} & Q_{c,k} & R_{c,k} \end{pmatrix}^T \tag{3.14}$$

Since the $\mathbf{r}_{c,k}^0$ vector is denoted as the cross product of $\mathbf{I}_{c,k}^0$ and $\mathbf{u}_k^0$, by using the skew symmetric matrix of $\mathbf{I}_{c,k}^0$ i.e. $\widehat{\mathbf{I}}_{c,k}^0$ and multiply it by $\mathbf{u}_k^0$ vector $P_{c,k}$, $Q_{c,k}$ and $R_{c,k}$ can be calculated as follows:

$$\widehat{\mathbf{I}}_{c,k}^{0}\cdot\mathbf{u}_{k}^{0}=\begin{bmatrix}0 & -z_{c,k} & y_{c,k}\\ z_{c,k} & 0 & -x_{c,k}\\ -y_{c,k} & x_{c,k} & 0\end{bmatrix}\cdot\begin{pmatrix}L_k\\ M_k\\ N_k\end{pmatrix}=\begin{pmatrix}-z_{c,k}M_k+y_{c,k}N_k\\ +z_{c,k}L_k-x_{c,k}N_k\\ -y_{c,k}L_k+x_{c,k}M_k\end{pmatrix} \qquad (3.15)$$

So

$$P_{c,k}=z_{c,k}\sin\varphi_k+y_{c,k}\cos\varphi_k \qquad (3.16)$$

Since $M_k=-\sin\varphi_k$ and $N_k=\cos\varphi_k$ and $Q_{c,k}=R_{c,k}=0$ since $L_k=x_{c,k}=0$. (x_k,y_k,z_k) trinaries are function of d_n (gear pitch diameters) and A_n (distances) which are measured between the gears and the fixed frame origins.

For the desired mechanism in Figure 3.1, the components of screw, which are defined above, are specified in terms of d_n ($n=1,2,3,4,5,6,7',\text{and } 7''$) and A_n ($n=1,2,\text{ and } 3$) as below and the pairs' coordinates for the sample GRM with 4 cycles are indicated in Table 1. Angles between fixed frame's z-axis and z-axes of revolute pairs are: $\varphi_8=\varphi_9=\varphi_{10}=\varphi_{13}=0$ and $\varphi_{11}=\varphi_{12}=\varphi_{14}=-90°$. So unit vectors of revolute joints w.r.t reference frame can be obtained by Eq. (3.7):

$$\mathbf{u}_8^0=\mathbf{u}_9^0=\mathbf{u}_{10}^0=\mathbf{u}_{13}^0=\begin{pmatrix}0 & 0 & 1\end{pmatrix}^T \text{ and } \mathbf{u}_{11}^0=\mathbf{u}_{12}^0=\mathbf{u}_{14}^0=\begin{pmatrix}0 & 1 & 0\end{pmatrix}^T.$$

Along each cycle, by using Table 1 and Eq. (3.16) the coefficients $P_{c,k}$ are defined as follows:

Cycle C_{15}:

$$P_{15,8}=z_{15,8}\sin\varphi_8+y_{15,8}\cos\varphi_8=z_{15,8}(\sin(0))+y_{15,8}(\cos(0))$$
$$=z_{15,8}(0)+y_{15,8}(1)=y_{15,8}=y_8-y_{15}=-\frac{d_4}{2}$$

$$P_{15,10}=z_{15,10}\sin\varphi_{10}+y_{15,10}\cos\varphi_{10}=z_{15,10}(\sin(0))+y_{15,10}(\cos(0))$$
$$=z_{15,10}(0)+y_{15,10}(1)=y_{15,10}=y_{10}-y_{15}=\frac{d_1}{2}$$

$P_{15,15}=0: y_{15,15}$ and $z_{15,15}=0$;

Cycle C_{16}:

$$P_{16,9} = z_{16,9}\sin\varphi_9 + y_{16,9}\cos\varphi_9 = z_{16,9}(\sin(0)) + y_{16,9}(\cos(0))$$
$$= z_{16,9}(0) + y_{16,9}(1) = y_{16,9} = y_9 - y_{16} = \frac{d_5}{2}$$

$$P_{16,10} = z_{16,10}\sin\varphi_{10} + y_{16,10}\cos\varphi_{10} = z_{16,10}(\sin(0)) + y_{16,10}(\cos(0))$$
$$= z_{16,10}(0) + y_{16,10}(1) = y_{16,10} = y_{10} - y_{16} = \frac{d_5}{2}$$

$$P_{16,12} = z_{16,12}\sin\varphi_{12} + y_{16,12}\cos\varphi_{12} = z_{16,12}(\sin(-90^\circ)) + y_{16,12}(\cos(-90^\circ))$$
$$= z_{16,12}(-1) + y_{16,12}(0) = -z_{16,12} = z_{16} - z_{12} = -\frac{d_2}{2}$$

$P_{16,16} = 0: y_{16,16}$ and $z_{16,16} = 0$;

Cycle C_{17}:

$$P_{17,11} = z_{17,11}\sin\varphi_{11} + y_{17,11}\cos\varphi_{11} = z_{17,11}(\sin(-90^\circ)) + y_{17,11}(\cos(-90^\circ))$$
$$= z_{17,11}(-1) + y_{17,11}(0) = -z_{17,11} = z_{17} - z_{11} = \frac{d_6}{2}$$

$$P_{17,12} = z_{17,12}\sin\varphi_{12} + y_{17,12}\cos\varphi_{12} = z_{17,12}(\sin(-90^\circ)) + y_{17,12}(\cos(-90^\circ))$$
$$= z_{17,12}(-1) + y_{17,12}(0) = -z_{17,12} = z_{17} - z_{12} = \frac{d_6}{2}$$

$$P_{17,13} = z_{17,13}\sin\varphi_{13} + y_{17,13}\cos\varphi_{13} = z_{17,13}(\sin(0)) + y_{17,13}(\cos(0))$$
$$= z_{17,13}(0) + y_{17,13}(1) = y_{17,13} = y_{13} - y_{17} = -\frac{d_7'}{2}$$

$P_{17,17} = 0: y_{17,17}$ and $z_{17,17} = 0$;

Cycle C_{18}:

$$P_{18,13} = z_{18,13}\sin\varphi_{13} + y_{18,13}\cos\varphi_{13} = z_{18,13}(\sin(0)) + y_{18,13}(\cos(0))$$
$$= z_{18,13}(0) + y_{18,13}(1) = y_{18,13} = y_{13} - y_{18} = -\frac{d_7''}{2}$$

$$P_{18,14} = z_{18,14}\sin\varphi_{14} + y_{18,14}\cos\varphi_{14} = z_{18,14}(\sin(-90^\circ)) + y_{18,14}(\cos(-90^\circ))$$
$$= z_{18,14}(-1) + y_{18,14}(0) = -z_{18,14} = z_{18} - z_{14} = -\frac{d_3}{2}$$

$P_{18,18} = 0: y_{18,18}$ and $z_{18,18} = 0$

Table 1: Coordinates of turning and gear pairs

	8	9	10	11	12	13	14	15	16	17	18
x_k	0	0	0	0	0	0	0	0	0	0	0
y_k	$-(d_1+d_4)/2$	0	0	B_2	B_1	0	B_1	$-d_1/2$	$-d_5/2$	$d_7'/2$	$d_7''/2$
z_k	0	0	$A_1-d_2/2$	A_1	A_1	A_2	A_3	0	$A_1-d_2/2$	$A_1+d_6/2$	$A_3-d_3/2$

After expressing all of the turning pairs screws, it is necessary to define velocity variables ($\dot{q} = \dot{\theta}$ or $\dot{d}$), for each revolute pair. In sample mechanism which is shown in Figure 3.1, because there exists just pure rotational displacement without any translational movement in mechanism's components (gears and carriers), there will be just angular velocity $\dot{\theta}_k$. Furthermore, *pitch*, which is stated as a ratio between the angular and linear velocities, will be zero. $\dot{\theta}_k$ is defined as a scalar which measures the rotational movement of the head link w.r.t tail link.

Twist about each screw points out the velocity as an angular velocity around the screw and linear velocity along the screw. The product between screw and velocity variables can be defined as a twist:

$$\hat{\mathbf{s}}_k^0 = \hat{\mathbf{u}}_{c,k}^0 \cdot \dot{\theta}_k = \begin{pmatrix} \mathbf{u}_k^0 \\ \hline \mathbf{I}_{c,k}^0 \times \mathbf{u}_k^0 \end{pmatrix} \cdot \dot{\theta}_k = \begin{pmatrix} \dot{\theta}_k \\ \hline \mathbf{I}_{c,k}^0 \times \dot{\theta}_k \end{pmatrix} \tag{3.17}$$

It can be noticed that in Eq. (3.17) there exist a dual vector. First is an angular velocity (rotation about screw) and second is linear velocity (sliding motion along screw). These two vectors are orthogonal to each other thus the projection of the linear part along the screw is zero and then the pitch will be zero as well. $\dot{\boldsymbol{\theta}}_{k,1}$ in Eq. (3.18) is twist intensities $k \times 1$ matrix which its entries are relative velocities of turning and gear pairs:

$$\dot{\boldsymbol{\theta}}_{k,1} = \begin{pmatrix} \dot{\theta}_t \\ \hline \dot{\theta}_c \end{pmatrix} \tag{3.18}$$

This matrix can be divided into two sub-matrices, one for entries related to turning pairs $\dot{\theta}_t$ and the other for entries corresponding to gear pairs $\dot{\theta}_c$. Since *k* edges indicate the relative movement between the tail link and head so angular velocities of pairs can be:

$$\dot{\theta}_k = \dot{\theta}_{n_{head}/n_{tail}} \tag{3.19}$$

In Figure 3.1, for example, the twist intensities matrix is

$$\dot{\boldsymbol{\theta}}_{11,1} = \left(\dot{\theta}_8 \quad \dot{\theta}_9 \quad \dot{\theta}_{10} \quad \dot{\theta}_{11} \quad \dot{\theta}_{12} \quad \dot{\theta}_{13} \quad \dot{\theta}_{14} \;\vdots\; \dot{\theta}_{15} \quad \dot{\theta}_{16} \quad \dot{\theta}_{17} \quad \dot{\theta}_{18}\right)^T \tag{3.20}$$

where $\dot{\boldsymbol{\theta}}_t = \left(\dot{\theta}_8 \quad \dot{\theta}_9 \quad \dot{\theta}_{10} \quad \dot{\theta}_{11} \quad \dot{\theta}_{12} \quad \dot{\theta}_{13} \quad \dot{\theta}_{14}\right)^T$ and $\dot{\boldsymbol{\theta}}_c = \left(\dot{\theta}_{15} \quad \dot{\theta}_{16} \quad \dot{\theta}_{17} \quad \dot{\theta}_{18}\right)^T$ are revolute and gear pairs twist intensities respectively. In addition, pairs' velocities are:

$$\begin{aligned}
&\dot{\theta}_8 = \dot{\theta}_{4/0}\,;\dot{\theta}_9 = \dot{\theta}_{5/0}\,;\dot{\theta}_{10} = \dot{\theta}_{1/0}\,;\dot{\theta}_{11} = \dot{\theta}_{6/1}\,;\\
&\dot{\theta}_{12} = \dot{\theta}_{2/1}\,;\dot{\theta}_{13} = \dot{\theta}_{7/2}\,;\dot{\theta}_{14} = \dot{\theta}_{3/2}\,;\dot{\theta}_{15} = \dot{\theta}_{1/4}\,;\\
&\dot{\theta}_{16} = \dot{\theta}_{2/5}\,;\dot{\theta}_{17} = \dot{\theta}_{7/6}\,;\dot{\theta}_{18} = \dot{\theta}_{3/7}.
\end{aligned} \tag{3.21}$$

By applying Hadamard entry-wise product on cycle-basis $\mathbf{C}$ and screw $\hat{\mathbf{u}}^0_{c,k}$ matrices given by Eq. (3.5) and (3.6), which have same dimension, Eq. (3.22) is obtained which is pointed out the relative angular velocities equations:

$$[\mathbf{C} \circ \hat{\mathbf{u}}^0_{c,k}\,] \cdot \dot{\boldsymbol{\theta}}_{k,1} = \mathbf{0}_{c,1} \tag{3.22}$$

where $\mathbf{0}_{c,1}$ is a column matrix with all zero entries. For sample mechanism in Figure 3.1, these equations are defined in Eq. (3.23):

$$\left[\begin{array}{cccccccc:cccc}
1\cdot\left(\frac{\mathbf{u}_8^0}{\mathbf{I}_{15,8}^0\times\mathbf{u}_8^0}\right) & 0\cdot\left(\frac{\mathbf{u}_9^0}{\mathbf{I}_{15,9}^0\times\mathbf{u}_9^0}\right) & -1\cdot\left(\frac{\mathbf{u}_{10}^0}{\mathbf{I}_{15,10}^0\times\mathbf{u}_{10}^0}\right) & 0\cdot\left(\frac{\mathbf{u}_{11}^0}{\mathbf{I}_{15,11}^0\times\mathbf{u}_{11}^0}\right) & 0\cdot\left(\frac{\mathbf{u}_{12}^0}{\mathbf{I}_{15,12}^0\times\mathbf{u}_{12}^0}\right) & 0\cdot\left(\frac{\mathbf{u}_{13}^0}{\mathbf{I}_{15,13}^0\times\mathbf{u}_{13}^0}\right) & 0\cdot\left(\frac{\mathbf{u}_{14}^0}{\mathbf{I}_{15,14}^0\times\mathbf{u}_{14}^0}\right) & 1\cdot\left(\frac{\mathbf{u}_{15}^0}{\mathbf{I}_{15,15}^0\times\mathbf{u}_{15}^0}\right) & 0\cdot\left(\frac{\mathbf{u}_{16}^0}{\mathbf{I}_{15,16}^0\times\mathbf{u}_{16}^0}\right) & 0\cdot\left(\frac{\mathbf{u}_{17}^0}{\mathbf{I}_{15,17}^0\times\mathbf{u}_{17}^0}\right) & 0\cdot\left(\frac{\mathbf{u}_{18}^0}{\mathbf{I}_{15,18}^0\times\mathbf{u}_{18}^0}\right) \\
0\cdot\left(\frac{\mathbf{u}_8^0}{\mathbf{I}_{16,8}^0\times\mathbf{u}_8^0}\right) & 1\cdot\left(\frac{\mathbf{u}_9^0}{\mathbf{I}_{16,9}^0\times\mathbf{u}_9^0}\right) & -1\cdot\left(\frac{\mathbf{u}_{10}^0}{\mathbf{I}_{16,10}^0\times\mathbf{u}_{10}^0}\right) & 0\cdot\left(\frac{\mathbf{u}_{11}^0}{\mathbf{I}_{16,11}^0\times\mathbf{u}_{11}^0}\right) & -1\cdot\left(\frac{\mathbf{u}_{12}^0}{\mathbf{I}_{16,12}^0\times\mathbf{u}_{12}^0}\right) & 0\cdot\left(\frac{\mathbf{u}_{13}^0}{\mathbf{I}_{16,13}^0\times\mathbf{u}_{13}^0}\right) & 0\cdot\left(\frac{\mathbf{u}_{14}^0}{\mathbf{I}_{16,14}^0\times\mathbf{u}_{14}^0}\right) & 0\cdot\left(\frac{\mathbf{u}_{15}^0}{\mathbf{I}_{16,15}^0\times\mathbf{u}_{15}^0}\right) & 1\cdot\left(\frac{\mathbf{u}_{16}^0}{\mathbf{I}_{16,16}^0\times\mathbf{u}_{16}^0}\right) & 0\cdot\left(\frac{\mathbf{u}_{17}^0}{\mathbf{I}_{16,17}^0\times\mathbf{u}_{17}^0}\right) & 0\cdot\left(\frac{\mathbf{u}_{18}^0}{\mathbf{I}_{16,18}^0\times\mathbf{u}_{18}^0}\right) \\
0\cdot\left(\frac{\mathbf{u}_8^0}{\mathbf{I}_{17,8}^0\times\mathbf{u}_8^0}\right) & 0\cdot\left(\frac{\mathbf{u}_9^0}{\mathbf{I}_{17,9}^0\times\mathbf{u}_9^0}\right) & 0\cdot\left(\frac{\mathbf{u}_{10}^0}{\mathbf{I}_{17,10}^0\times\mathbf{u}_{10}^0}\right) & 1\cdot\left(\frac{\mathbf{u}_{11}^0}{\mathbf{I}_{17,11}^0\times\mathbf{u}_{11}^0}\right) & -1\cdot\left(\frac{\mathbf{u}_{12}^0}{\mathbf{I}_{17,12}^0\times\mathbf{u}_{12}^0}\right) & -1\cdot\left(\frac{\mathbf{u}_{13}^0}{\mathbf{I}_{17,13}^0\times\mathbf{u}_{13}^0}\right) & 0\cdot\left(\frac{\mathbf{u}_{14}^0}{\mathbf{I}_{17,14}^0\times\mathbf{u}_{14}^0}\right) & 0\cdot\left(\frac{\mathbf{u}_{15}^0}{\mathbf{I}_{17,15}^0\times\mathbf{u}_{15}^0}\right) & 0\cdot\left(\frac{\mathbf{u}_{16}^0}{\mathbf{I}_{17,16}^0\times\mathbf{u}_{16}^0}\right) & 1\cdot\left(\frac{\mathbf{u}_{17}^0}{\mathbf{I}_{17,17}^0\times\mathbf{u}_{17}^0}\right) & 0\cdot\left(\frac{\mathbf{u}_{18}^0}{\mathbf{I}_{17,18}^0\times\mathbf{u}_{18}^0}\right) \\
0\cdot\left(\frac{\mathbf{u}_8^0}{\mathbf{I}_{18,8}^0\times\mathbf{u}_8^0}\right) & 0\cdot\left(\frac{\mathbf{u}_9^0}{\mathbf{I}_{18,9}^0\times\mathbf{u}_9^0}\right) & 0\cdot\left(\frac{\mathbf{u}_{10}^0}{\mathbf{I}_{18,10}^0\times\mathbf{u}_{10}^0}\right) & 0\cdot\left(\frac{\mathbf{u}_{11}^0}{\mathbf{I}_{18,11}^0\times\mathbf{u}_{11}^0}\right) & 0\cdot\left(\frac{\mathbf{u}_{12}^0}{\mathbf{I}_{18,12}^0\times\mathbf{u}_{12}^0}\right) & 1\cdot\left(\frac{\mathbf{u}_{13}^0}{\mathbf{I}_{18,13}^0\times\mathbf{u}_{13}^0}\right) & -1\cdot\left(\frac{\mathbf{u}_{14}^0}{\mathbf{I}_{18,14}^0\times\mathbf{u}_{14}^0}\right) & 0\cdot\left(\frac{\mathbf{u}_{15}^0}{\mathbf{I}_{18,15}^0\times\mathbf{u}_{15}^0}\right) & 0\cdot\left(\frac{\mathbf{u}_{16}^0}{\mathbf{I}_{18,16}^0\times\mathbf{u}_{16}^0}\right) & 0\cdot\left(\frac{\mathbf{u}_{17}^0}{\mathbf{I}_{18,17}^0\times\mathbf{u}_{17}^0}\right) & 0\cdot\left(\frac{\mathbf{u}_{18}^0}{\mathbf{I}_{17,18}^0\times\mathbf{u}_{18}^0}\right)
\end{array}\right]\cdot\left(\begin{array}{c}
\dot{\theta}_8 \\ \dot{\theta}_9 \\ \dot{\theta}_{10} \\ \dot{\theta}_{11} \\ \dot{\theta}_{12} \\ \dot{\theta}_{13} \\ \dot{\theta}_{14} \\ \hdashline \dot{\theta}_{15} \\ \dot{\theta}_{16} \\ \dot{\theta}_{17} \\ \dot{\theta}_{18}
\end{array}\right)=\left(\begin{array}{c}0\\0\\0\\0\end{array}\right)$$

(3.23)

The orthogonality conditions for relative velocities and relative velocity moments must be satisfied in order to Eq. (3.23) holds true:

- The sum of $\dot{\boldsymbol{\theta}}_k$ (twist intensities) in each cycle in the cycle basis must equal to zero.

Since $\dot{\boldsymbol{\theta}}_k = \boldsymbol{\omega}^0_{head} - \boldsymbol{\omega}^0_{tail}$ so in each cycle each absolute velocity $\boldsymbol{\omega}^0_{head}$ and $\boldsymbol{\omega}^0_{tail}$ will appear twice with opposite sign so the sum will be zero.

According to orthogonality condition for relative velocities, Eq. (3.24) can be written for sample mechanism in Figure 3.1. As it was discussed in Section 3.2, the desired mechanism has 4 fundamental circuits hence Eq. (3.24) can just express equations of these f-circuits such that each row illustrates relations between the relative angular velocities of turning pairs and gear pair corresponding to each cycle. Actually, if the relative angular velocity of gear pairs at the contact point of two gears is desired, it will be necessary to use Eq. (3.24) in order to acquire these velocities in terms of input angular velocities.

$$\left[\begin{array}{ccccccc:cccc} 1\cdot\mathbf{u}_8^0 & 0\cdot\mathbf{u}_9^0 & -1\cdot\mathbf{u}_{10}^0 & 0\cdot\mathbf{u}_{11}^0 & 0\cdot\mathbf{u}_{12}^0 & 0\cdot\mathbf{u}_{13}^0 & 0\cdot\mathbf{u}_{14}^0 & 1\cdot\mathbf{u}_{15}^0 & 0\cdot\mathbf{u}_{16}^0 & 0\cdot\mathbf{u}_{17}^0 & 0\cdot\mathbf{u}_{18}^0 \\ 0\cdot\mathbf{u}_8^0 & 1\cdot\mathbf{u}_9^0 & -1\cdot\mathbf{u}_{10}^0 & 0\cdot\mathbf{u}_{11}^0 & -1\cdot\mathbf{u}_{12}^0 & 0\cdot\mathbf{u}_{13}^0 & 0\cdot\mathbf{u}_{14}^0 & 0\cdot\mathbf{u}_{15}^0 & 1\cdot\mathbf{u}_{16}^0 & 0\cdot\mathbf{u}_{17}^0 & 0\cdot\mathbf{u}_{18}^0 \\ 0\cdot\mathbf{u}_8^0 & 0\cdot\mathbf{u}_9^0 & 0\cdot\mathbf{u}_{10}^0 & 1\cdot\mathbf{u}_{11}^0 & -1\cdot\mathbf{u}_{12}^0 & -1\cdot\mathbf{u}_{13}^0 & 0\cdot\mathbf{u}_{14}^0 & 0\cdot\mathbf{u}_{15}^0 & 0\cdot\mathbf{u}_{16}^0 & 1\cdot\mathbf{u}_{17}^0 & 0\cdot\mathbf{u}_{18}^0 \\ 0\cdot\mathbf{u}_8^0 & 0\cdot\mathbf{u}_9^0 & 0\cdot\mathbf{u}_{10}^0 & 0\cdot\mathbf{u}_{11}^0 & 0\cdot\mathbf{u}_{12}^0 & 1\cdot\mathbf{u}_{13}^0 & -1\cdot\mathbf{u}_{14}^0 & 0\cdot\mathbf{u}_{15}^0 & 0\cdot\mathbf{u}_{16}^0 & 0\cdot\mathbf{u}_{17}^0 & 1\cdot\mathbf{u}_{18}^0 \end{array}\right] \cdot \begin{pmatrix} \dot{\theta}_8 \\ \dot{\theta}_9 \\ \dot{\theta}_{10} \\ \dot{\theta}_{11} \\ \dot{\theta}_{12} \\ \dot{\theta}_{13} \\ \dot{\theta}_{14} \\ \dot{\theta}_{15} \\ \dot{\theta}_{16} \\ \dot{\theta}_{17} \\ \dot{\theta}_{18} \end{pmatrix} = \begin{pmatrix} 0 \\ 0 \\ 0 \\ 0 \end{pmatrix} \tag{3.24}$$

- The sum of $\mathbf{I}^{0}_{c,k} \times \dot{\boldsymbol{\theta}}_{k}$ (moments of relative velocities) in each cycle in the cycle basis must equal to zero w.r.t gear pair *c*.

Since the sum of twist intensities, according to previous condition, is zero in each cycle so $\dot{\boldsymbol{\theta}}_{c}$ can be defined as the resultant twist of the turning twists $\dot{\boldsymbol{\theta}}_{t}$. Because $\mathbf{I}^{0}_{c,k}$ of the twist resultant is zero so the moment of that will be zero as well. Therefore, the sum of the moment of the turning twists will be also zero.

Again, according to orthogonality condition for moments of relative velocities, Eq. (3.25) can be written for desired mechanism in Figure 3.1.

$$\left[\begin{array}{cccccccc:cccc}
1\cdot\begin{pmatrix}P_{15,8}\\Q_{15,8}\\R_{15,8}\end{pmatrix} & 0\cdot\begin{pmatrix}P_{15,9}\\Q_{15,9}\\R_{15,9}\end{pmatrix} & -1\cdot\begin{pmatrix}P_{15,10}\\Q_{15,10}\\R_{15,10}\end{pmatrix} & 0\cdot\begin{pmatrix}P_{15,11}\\Q_{15,11}\\R_{15,11}\end{pmatrix} & 0\cdot\begin{pmatrix}P_{15,12}\\Q_{15,12}\\R_{15,12}\end{pmatrix} & 0\cdot\begin{pmatrix}P_{15,13}\\Q_{15,13}\\R_{15,13}\end{pmatrix} & 0\cdot\begin{pmatrix}P_{15,14}\\Q_{15,14}\\R_{15,14}\end{pmatrix} & 1\cdot\begin{pmatrix}P_{15,15}\\Q_{15,15}\\R_{15,15}\end{pmatrix} & 0\cdot\begin{pmatrix}P_{15,16}\\Q_{15,16}\\R_{15,16}\end{pmatrix} & 0\cdot\begin{pmatrix}P_{15,17}\\Q_{15,17}\\R_{15,17}\end{pmatrix} & 0\cdot\begin{pmatrix}P_{15,18}\\Q_{15,18}\\R_{15,18}\end{pmatrix} \\
0\cdot\begin{pmatrix}P_{16,8}\\Q_{16,8}\\R_{16,8}\end{pmatrix} & 1\cdot\begin{pmatrix}P_{16,9}\\Q_{16,9}\\R_{16,9}\end{pmatrix} & -1\cdot\begin{pmatrix}P_{16,10}\\Q_{16,10}\\R_{16,10}\end{pmatrix} & 0\cdot\begin{pmatrix}P_{16,11}\\Q_{16,11}\\R_{16,11}\end{pmatrix} & -1\cdot\begin{pmatrix}P_{16,12}\\Q_{16,12}\\R_{16,12}\end{pmatrix} & 0\cdot\begin{pmatrix}P_{16,13}\\Q_{16,13}\\R_{16,13}\end{pmatrix} & 0\cdot\begin{pmatrix}P_{16,14}\\Q_{16,14}\\R_{16,14}\end{pmatrix} & 0\cdot\begin{pmatrix}P_{16,15}\\Q_{16,15}\\R_{16,15}\end{pmatrix} & 1\cdot\begin{pmatrix}P_{16,16}\\Q_{16,16}\\R_{16,16}\end{pmatrix} & 0\cdot\begin{pmatrix}P_{16,17}\\Q_{16,17}\\R_{16,17}\end{pmatrix} & 0\cdot\begin{pmatrix}P_{16,18}\\Q_{16,18}\\R_{16,18}\end{pmatrix} \\
0\cdot\begin{pmatrix}P_{17,8}\\Q_{17,8}\\R_{17,8}\end{pmatrix} & 0\cdot\begin{pmatrix}P_{17,9}\\Q_{17,9}\\R_{17,9}\end{pmatrix} & 0\cdot\begin{pmatrix}P_{17,10}\\Q_{17,10}\\R_{17,10}\end{pmatrix} & 1\cdot\begin{pmatrix}P_{17,11}\\Q_{17,11}\\R_{17,11}\end{pmatrix} & -1\cdot\begin{pmatrix}P_{17,12}\\Q_{17,12}\\R_{17,12}\end{pmatrix} & -1\cdot\begin{pmatrix}P_{17,13}\\Q_{17,13}\\R_{17,13}\end{pmatrix} & 0\cdot\begin{pmatrix}P_{17,14}\\Q_{17,14}\\R_{17,14}\end{pmatrix} & 0\cdot\begin{pmatrix}P_{17,15}\\Q_{17,15}\\R_{17,15}\end{pmatrix} & 0\cdot\begin{pmatrix}P_{17,16}\\Q_{17,16}\\R_{17,16}\end{pmatrix} & 1\cdot\begin{pmatrix}P_{17,17}\\Q_{17,17}\\R_{17,17}\end{pmatrix} & 0\cdot\begin{pmatrix}P_{17,18}\\Q_{17,18}\\R_{17,18}\end{pmatrix} \\
0\cdot\begin{pmatrix}P_{18,8}\\Q_{18,8}\\R_{18,8}\end{pmatrix} & 0\cdot\begin{pmatrix}P_{18,9}\\Q_{18,9}\\R_{18,9}\end{pmatrix} & 0\cdot\begin{pmatrix}P_{18,10}\\Q_{18,10}\\R_{18,10}\end{pmatrix} & 0\cdot\begin{pmatrix}P_{18,11}\\Q_{18,11}\\R_{18,11}\end{pmatrix} & 0\cdot\begin{pmatrix}P_{18,12}\\Q_{18,12}\\R_{18,12}\end{pmatrix} & 1\cdot\begin{pmatrix}P_{18,13}\\Q_{18,13}\\R_{18,13}\end{pmatrix} & -1\cdot\begin{pmatrix}P_{18,14}\\Q_{18,14}\\R_{18,14}\end{pmatrix} & 0\cdot\begin{pmatrix}P_{18,15}\\Q_{18,15}\\R_{18,15}\end{pmatrix} & 0\cdot\begin{pmatrix}P_{18,16}\\Q_{18,16}\\R_{18,16}\end{pmatrix} & 0\cdot\begin{pmatrix}P_{18,17}\\Q_{18,17}\\R_{18,17}\end{pmatrix} & 1\cdot\begin{pmatrix}P_{18,18}\\Q_{18,18}\\R_{18,18}\end{pmatrix}
\end{array}\right]\cdot\begin{pmatrix}\dot{\theta}_8\\\dot{\theta}_9\\\dot{\theta}_{10}\\\dot{\theta}_{11}\\\dot{\theta}_{12}\\\dot{\theta}_{13}\\\dot{\theta}_{14}\\\dot{\theta}_{15}\\\dot{\theta}_{16}\\\dot{\theta}_{17}\\\dot{\theta}_{18}\end{pmatrix}=\begin{pmatrix}0\\0\\0\\0\end{pmatrix} \qquad (3.25)$$

In Eq. (3.25) according to Eq. (3.15) all $Q_{c,k}$ and $R_{c,k}$ entries will be zero and from Eq. (3.13) $P_{15,15}$, $P_{16,16}$, $P_{17,17}$, and $P_{18,18} = 0$ as well.

3.2.3 Independent Equations for Relative Velocities of Turning Pairs

The Eq. (3.25) can be written in the following form:

$$\left[\mathbf{P}_{c,t} \mid \mathbf{0}_{c,c}\right] \cdot \begin{pmatrix} \dot{\boldsymbol{\theta}}_t \\ \hline \dot{\boldsymbol{\theta}}_c \end{pmatrix} = \left(\mathbf{0}_c\right) \tag{3.26}$$

As it was shown above, by Hadamard entry-wise product of cycle-basis and screw matrices, relative angular velocities are obtained. After substituting the parameters, the $\left[\mathbf{P}_{c,t} \mid \mathbf{0}_{c,c}\right]$ is acquired which has two sub-matrices: the $c \times t$ Coefficient matrix $\mathbf{P}$ and the $c \times c$ zero matrix. Here, the coefficient matrix is defined as following:

$$\mathbf{P}_{c,t} = \left[\mathbf{T} \circ \hat{\mathbf{u}}_k^0\right] \tag{3.27}$$

where $\mathbf{T}$ and $\hat{\mathbf{u}}_k^0$ are $c \times t$ spanning tree and screw matrices defined in Eq. (3.4) and (3.6) respectively.

By row-column operations, one can obtain independent equations for relative angular velocities of only turning pairs. Since rank of Matroid is invariant to these operations, *c* independent equations are made by them. Deleting columns and rows with all zero entries as row-column operations are allowed for any Matroid. In Eq. (3.25), by deleting zero rows where are related to $Q_{c,k}$ and $R_{c,k}$ entries and zero columns 15, 16, 17, and 18 and corresponding $\dot{\boldsymbol{\theta}}_c$ entries, Eq. (3.26) can be simplified to the following form:

$$\left[\mathbf{P}_{c,t}\right] \cdot \left(\dot{\boldsymbol{\theta}}_t\right) = \left(\mathbf{0}_c\right) \tag{3.28}$$

For sample mechanism in Figure 3.1, Eq. (3.28) can be written as follows:

$$\begin{bmatrix} P_{15,8} & 0 & -P_{15,10} & 0 & 0 & 0 & 0 \\ 0 & P_{16,9} & -P_{16,10} & 0 & -P_{16,12} & 0 & 0 \\ 0 & 0 & 0 & P_{17,11} & -P_{17,12} & -P_{17,13} & 0 \\ 0 & 0 & 0 & 0 & 0 & P_{18,13} & -P_{18,14} \end{bmatrix} \cdot \begin{pmatrix} \dot{\theta}_8 \\ \dot{\theta}_9 \\ \dot{\theta}_{10} \\ \dot{\theta}_{11} \\ \dot{\theta}_{12} \\ \dot{\theta}_{13} \\ \dot{\theta}_{14} \end{pmatrix} = \begin{pmatrix} 0 \\ 0 \\ 0 \\ 0 \end{pmatrix} \quad (3.29)$$

Eq. (3.29) is a final result for independent equations of relative angular velocities and $P_{c,t}$ are scalar coefficients. These equations have an analogy with Willis equations but Willis equations are used in absolute angular velocities as scalar equations.

Substituting values of $P_{c,t}$ in Eq. (3.29) yields below equations which express relative velocities in terms of pitch diameter d_n:

$$\begin{bmatrix} -\frac{d_4}{2} & 0 & -\frac{d_1}{2} & 0 & 0 & 0 & 0 \\ 0 & \frac{d_5}{2} & -\frac{d_5}{2} & 0 & \frac{d_2}{2} & 0 & 0 \\ 0 & 0 & 0 & \frac{d_6}{2} & -\frac{d_6}{2} & \frac{d_7'}{2} & 0 \\ 0 & 0 & 0 & 0 & 0 & -\frac{d_7''}{2} & \frac{d_3}{2} \end{bmatrix} \cdot \begin{pmatrix} \dot{\theta}_8 \\ \dot{\theta}_9 \\ \dot{\theta}_{10} \\ \dot{\theta}_{11} \\ \dot{\theta}_{12} \\ \dot{\theta}_{13} \\ \dot{\theta}_{14} \end{pmatrix} = \begin{pmatrix} 0 \\ 0 \\ 0 \\ 0 \end{pmatrix} \quad (3.30)$$

Since Eq. (3.30) is written in terms of pitch diameters, one can point it out as functions of tooth ratio. It is a positive number for each meshing joint *c*. Indeed, in digraph *D* it is weight of edge *c* where *tail* and *head* links are connected together:

$$i_c = \frac{d_{n_t}}{d_{n_h}} = \frac{N_{n_t}}{N_{n_h}} \quad (3.31)$$

where N_{n_t} and d_{n_t} are the number of teeth and pitch diameter of input gear and N_{n_h} and d_{n_h} are related to output gear. Each row of the $P_{c,t}$ matrix contains two pitch diameters one related input gear of gear pair and the other related to output gear of gear pair (according to dash line in each cycle). For writing this matrix in terms of

tooth ratio, each row must be divided by the pitch diameter of the output gear (the head node of the dash line in each cycle).

In Figure 3.1, for instance, following tooth ratios can be defined:

$$i_{15}=\frac{d_4}{d_1};i_{16}=\frac{d_5}{d_2};i_{17}=\frac{d_6}{d_7'};i_{18}=\frac{d_7''}{d_3} \tag{3.32}$$

3.2.4 Solution of Relative Velocities of Turning Pairs

Eq. (3.30) can be written in terms of tooth ratio so $\mathbf{A}_{c,t}$ matrix is obtained:

$$\left[\mathbf{A}_{c,t}\right]\cdot\left(\dot{\boldsymbol{\theta}}_t\right)=\left(\mathbf{0}_c\right) \tag{3.33}$$

According to Kutzbach criterion [46], the total number of Degree of Freedom (DOF) is expressed in Eq. (3.34):

$$E=3n-2t-r \tag{3.34}$$

where 3*n* is the total number of mobility and each turning joint and gear pair has one and two DOF respectively. As a result, in the case of gear trains because $t=n$, Eq. (3.34) will be

$$E=n-r \tag{3.35}$$

Eq. (3.35) states that there is a relation between DOF (E) i.e. input velocities (known variables), turning pairs $(t=n)$ and the rank of cycle-basis matrix (*r*) i.e. output velocities (unknown variables). In other words, from Eq. (3.35), it can be concluded that the number of turning pairs is equal to the summation of DOF and rank of cycle-basis matrix. In fact, in each mechanism, the number of input and output variables must be equal to the number of DOF and rank of $\mathbf{C}$ matrix respectively. In the sample mechanism, Figure 3.1, as it was said in Section 3.2 the number of input and output velocities are 3 and 4 respectively. Now, this statement can be verified since $E=3$ and $t=n=7$ and $r=4$.

According to the relations between number of links, fundamental cycles and DOF, Eq. (3.33) can be partitioned as following:

$$\left[\mathbf{A}_{r,E} \mid \mathbf{A}_{r,r}\right]\cdot\left(\begin{matrix}\dot{\boldsymbol{\theta}}_E \\ \hline \dot{\boldsymbol{\theta}}_r\end{matrix}\right)=\left(\mathbf{0}_r\right) \tag{3.36}$$

Hence, solutions for output relative velocities $\dot{\boldsymbol{\theta}}_r$ can be defined as functions of input relative velocities $\dot{\boldsymbol{\theta}}_E$:

$$\left(\dot{\boldsymbol{\theta}}_r\right)=-\left[\mathbf{A}_r\right]^{-1}\cdot\left[\mathbf{A}_E\right]\cdot\left(\dot{\boldsymbol{\theta}}_E\right) \tag{3.37}$$

Note that in digraph *D*, Figure 3.2, according to labeling since 8, 9, and 11 edges are considered as inputs, and outputs are determined by other edges i.e. 10, 12, 13, and 14, the order of third and fourth columns in $\mathbf{A}$ matrix and third and fourth rows in $\dot{\boldsymbol{\theta}}$ vector must be changed as in Eq. (3.38):

$$\left[\begin{array}{ccc:ccc:c}-i_{15} & 0 & 0 & -1 & 0 & 0 & 0 \\ 0 & +i_{16} & 0 & -i_{16} & +1 & 0 & 0 \\ 0 & 0 & +i_{17} & 0 & -i_{17} & +1 & 0 \\ 0 & 0 & 0 & 0 & 0 & -i_{18} & +1\end{array}\right]\cdot\left(\begin{matrix}\dot{\theta}_8 \\ \dot{\theta}_9 \\ \dot{\theta}_{11} \\ \hline \dot{\theta}_{10} \\ \dot{\theta}_{12} \\ \dot{\theta}_{13} \\ \dot{\theta}_{14}\end{matrix}\right)=\begin{pmatrix}0\\0\\0\\0\end{pmatrix} \tag{3.38}$$

$$\begin{pmatrix}\dot{\theta}_{10}\\ \dot{\theta}_{12}\\ \dot{\theta}_{13}\\ \dot{\theta}_{14}\end{pmatrix}=-\begin{bmatrix}-1 & 0 & 0 & 0\\ -i_{16} & +1 & 0 & 0\\ 0 & -i_{17} & +1 & 0\\ 0 & 0 & -i_{18} & +1\end{bmatrix}^{-1}\cdot\begin{bmatrix}-i_{15} & 0 & 0\\ 0 & +i_{16} & 0\\ 0 & 0 & +i_{17}\\ 0 & 0 & 0\end{bmatrix}\cdot\begin{pmatrix}\dot{\theta}_8\\ \dot{\theta}_9\\ \dot{\theta}_{11}\end{pmatrix} \tag{3.39}$$

$$\begin{pmatrix}\dot{\theta}_{10}\\ \dot{\theta}_{12}\\ \dot{\theta}_{13}\\ \dot{\theta}_{14}\end{pmatrix}=\begin{bmatrix}-i_{15} & 0 & 0\\ -i_{16}i_{15} & -i_{16} & 0\\ -i_{17}i_{16}i_{15} & -i_{17}i_{16} & -i_{17}\\ -i_{18}i_{17}i_{16}i_{15} & -i_{18}i_{17}i_{16} & -i_{18}i_{17}\end{bmatrix}\cdot\begin{pmatrix}\dot{\theta}_8\\ \dot{\theta}_9\\ \dot{\theta}_{11}\end{pmatrix} \tag{3.40}$$

Eq. (3.40) expresses the equations of output relative angular velocities in terms of input relative angular velocities. In the next section (Section 3.2.5), these equations

are used to determine absolute angular velocities of links.

3.2.5 Links Absolute Angular Velocities

$\boldsymbol{\omega}_n^0$ is $3n \times 1$ Absolute Velocity Matrix which has *n* vectorial entries (each entry is a 3-component vector) equal to the number of links.

$$\begin{aligned}\boldsymbol{\omega}^0 &= \begin{pmatrix}\boldsymbol{\omega}_1^0 & \boldsymbol{\omega}_2^0 & \cdots & \boldsymbol{\omega}_n^0\end{pmatrix}^T \\ &= \begin{pmatrix}\omega_1^{x_0} & \omega_1^{y_0} & \omega_1^{z_0} \mid \omega_2^{x_0} & \omega_2^{y_0} & \omega_2^{z_0} \mid \cdots \mid \omega_7^{x_0} & \omega_7^{y_0} & \omega_7^{z_0}\end{pmatrix}^T\end{aligned} \tag{3.41}$$

The entries of this matrix are the absolute velocities of links (vertices of digraph) of the mechanism (gears, carriers, and planets) w.r.t. reference frame. The differences between absolute velocities of head links $\boldsymbol{\omega}_{n_h}^0$ relative to tail links $\boldsymbol{\omega}_{n_h}^0$ yield relative velocities $\dot{\boldsymbol{\theta}}_k$:

$$\dot{\boldsymbol{\theta}}_k = \boldsymbol{\omega}_{n_h}^0 - \boldsymbol{\omega}_{n_t}^0 \tag{3.42}$$

For desired mechanism:

$$\begin{aligned}\boldsymbol{\omega}^0 &= \begin{pmatrix}\boldsymbol{\omega}_1^0 & \boldsymbol{\omega}_2^0 & \boldsymbol{\omega}_3^0 & \boldsymbol{\omega}_4^0 & \boldsymbol{\omega}_5^0 & \boldsymbol{\omega}_6^0 & \boldsymbol{\omega}_7^0\end{pmatrix}^T \\ &= \begin{pmatrix}\omega_1^{x_0} & \omega_1^{y_0} & \omega_1^{z_0} \mid \omega_2^{x_0} & \omega_2^{y_0} & \omega_2^{z_0} \mid \omega_3^{x_0} & \omega_3^{y_0} & \omega_3^{z_0} \mid \omega_4^{x_0} & \omega_4^{y_0} & \omega_4^{z_0} \mid \omega_5^{x_0} & \omega_5^{y_0} & \omega_5^{z_0} \mid \omega_6^{x_0} & \omega_6^{y_0} & \omega_6^{z_0} \mid \omega_7^{x_0} & \omega_7^{y_0} & \omega_7^{z_0}\end{pmatrix}^T\end{aligned}$$

(3.43)

Each absolute velocity $\boldsymbol{\omega}_n^0$ is produced by summing the relative velocities of turning pairs *t* which exist in path *n* from node 0 to node *n*. By using path matrix $\mathbf{Z}$, Eq. (3.3), and relative velocities of turning pairs, $\dot{\boldsymbol{\theta}}_t$, the absolute velocity matrix can be calculated as in Eq. (3.44):

$$\boldsymbol{\omega}_n^0 = -\left[\mathbf{Z}^T \circ \mathbf{u}_t^0\right] \cdot \left(\dot{\boldsymbol{\theta}}_t\right) \tag{3.44}$$

It is necessary to note that because links (nodes of digraph) velocities are desired, $\mathbf{Z}^T$ as an $n \times t$ transposed matrix of $\mathbf{Z}$, which connects the nodes-edges of spanning tree, is used. Moreover, since absolute velocities are vectorial quantities, Hadamard

entry-wise product of $\mathbf{Z}^T$ and unit vectors $\mathbf{u}_t^0$ defined in Eq. (3.7) (orientation of z-axis of each turning pair) is applied in order to determine that which relative velocities can have effect on each of absolute velocities and in which orientation w.r.t. fixed frame.

For Figure 3.1:

$$\begin{pmatrix} \omega_1^0 \\ \omega_2^0 \\ \omega_3^0 \\ \omega_4^0 \\ \omega_5^0 \\ \omega_6^0 \\ \omega_7^0 \end{pmatrix} = \begin{bmatrix} 0 & 0 & u_{10}^0 & 0 & 0 & 0 & 0 \\ 0 & 0 & u_{10}^0 & 0 & u_{12}^0 & 0 & 0 \\ 0 & 0 & u_{10}^0 & 0 & u_{12}^0 & 0 & u_{14}^0 \\ u_8^0 & 0 & 0 & 0 & 0 & 0 & 0 \\ 0 & u_9^0 & 0 & 0 & 0 & 0 & 0 \\ 0 & 0 & u_{10}^0 & u_{11}^0 & 0 & 0 & 0 \\ 0 & 0 & u_{10}^0 & 0 & u_{12}^0 & u_{13}^0 & 0 \end{bmatrix} \cdot \begin{pmatrix} \dot{\theta}_8 \\ \dot{\theta}_9 \\ \dot{\theta}_{10} \\ \dot{\theta}_{11} \\ \dot{\theta}_{12} \\ \dot{\theta}_{13} \\ \dot{\theta}_{14} \end{pmatrix} \tag{3.45}$$

By solving these equations vectorial absolute velocity of each link can be obtained:

- Angular velocity of ink 1 w.r.t. link 0: it has just z-component in terms of $\dot{\theta}_8$

$$\begin{aligned} \omega_1^0 &= u_{10}^0 \dot{\theta}_{10} \\ &= \begin{pmatrix} 0 \\ 0 \\ 1 \end{pmatrix} \dot{\theta}_{10} \\ &= \begin{pmatrix} 0 \\ 0 \\ -i_{15}\dot{\theta}_8 \end{pmatrix} \end{aligned} \tag{3.46}$$

- Angular velocity of link 2 w.r.t. link 0: it has y-component in terms of $\dot{\theta}_8$ and $\dot{\theta}_9$ and also z-component in terms of just $\dot{\theta}_8$

$$\begin{aligned} \omega_2^0 &= u_{10}^0 \dot{\theta}_{10} + u_{12}^0 \dot{\theta}_{12} \\ &= \begin{pmatrix} 0 \\ 0 \\ 1 \end{pmatrix} \dot{\theta}_{10} + \begin{pmatrix} 0 \\ 1 \\ 0 \end{pmatrix} \dot{\theta}_{12} \\ &= \begin{pmatrix} 0 \\ -i_{16}i_{15}\dot{\theta}_8 - i_{16}\dot{\theta}_9 \\ -i_{15}\dot{\theta}_8 \end{pmatrix} \end{aligned} \tag{3.47}$$

- Angular velocity of link 3 w.r.t. link0: it has y-component in terms of $\dot{\theta}_8$, $\dot{\theta}_9$, and $\dot{\theta}_{11}$ and also z-component in terms of just $\dot{\theta}_8$

$$\begin{aligned}\omega_3^0 &= u_{10}^0\dot{\theta}_{10} + u_{12}^0\dot{\theta}_{12} + u_{14}^0\dot{\theta}_{14} \\ &= \begin{pmatrix}0\\0\\1\end{pmatrix}\dot{\theta}_{10} + \begin{pmatrix}0\\1\\0\end{pmatrix}\dot{\theta}_{12} + \begin{pmatrix}0\\1\\0\end{pmatrix}\dot{\theta}_{14} \\ &= \begin{pmatrix}0\\-i_{16}i_{15}\left(i_{18}i_{17}+1\right)\dot{\theta}_8 - i_{16}\left(i_{18}i_{17}+1\right)\dot{\theta}_9 - i_{18}i_{17}\dot{\theta}_{11}\\-i_{15}\dot{\theta}_8\end{pmatrix}\end{aligned} \tag{3.48}$$

- Angular velocity of link 4 w.r.t. link 0 : it is one of input velocity ($\dot{\theta}_8$)

$$\begin{aligned}\omega_4^0 &= u_8^0\dot{\theta}_8 \\ &= \begin{pmatrix}0\\0\\1\end{pmatrix}\dot{\theta}_8 \\ &= \begin{pmatrix}0\\0\\\dot{\theta}_8\end{pmatrix}\end{aligned} \tag{3.49}$$

- Angular velocity of link 5 w.r.t. link 0: it is one of input velocity ($\dot{\theta}_9$)

$$\begin{aligned}\omega_5^0 &= u_9^0\dot{\theta}_9 \\ &= \begin{pmatrix}0\\0\\1\end{pmatrix}\dot{\theta}_9 \\ &= \begin{pmatrix}0\\0\\\dot{\theta}_9\end{pmatrix}\end{aligned} \tag{3.50}$$

- Angular velocity of link 6 w.r.t. link 0: it has y-component in terms of just $\dot{\theta}_{11}$ and also z-component in terms of just $\dot{\theta}_8$

$$\omega_6^0 = u_{10}^0\dot{\theta}_{10} + u_{11}^0\dot{\theta}_{11}$$

$$= \begin{pmatrix} 0 \\ 0 \\ 1 \end{pmatrix}\dot{\theta}_{10} + \begin{pmatrix} 0 \\ 1 \\ 0 \end{pmatrix}\dot{\theta}_{11} \tag{3.51}$$

$$= \begin{pmatrix} 0 \\ \dot{\theta}_{11} \\ -i_{15}\dot{\theta}_8 \end{pmatrix}$$

- Angular velocity of link 7 w.r.t. link 0: it has y-component in terms of $\dot{\theta}_8$ and $\dot{\theta}_9$ and also z-component in terms of input velocities ($\dot{\theta}_8$, $\dot{\theta}_9$, and $\dot{\theta}_{11}$)

$$\omega_7^0 = u_{10}^0\dot{\theta}_{10} + u_{12}^0\dot{\theta}_{12} + u_{13}^0\dot{\theta}_{13}$$

$$= \begin{pmatrix} 0 \\ 0 \\ 1 \end{pmatrix}\dot{\theta}_{10} + \begin{pmatrix} 0 \\ 1 \\ 0 \end{pmatrix}\dot{\theta}_{12} + \begin{pmatrix} 0 \\ 0 \\ 1 \end{pmatrix}\dot{\theta}_{13} \tag{3.52}$$

$$= \begin{pmatrix} 0 \\ -i_{16}i_{15}\dot{\theta}_8 - i_{16}\dot{\theta}_9 \\ -i_{15}(i_{17}i_{16}+1)\dot{\theta}_8 - i_{17}i_{16}\dot{\theta}_9 - i_{17}\dot{\theta}_{11} \end{pmatrix}$$

3.3 Kinematic Analysis Using T-T Graph

3.3.1 T-T Graph and Unkown Angular Velocities

The functional representation of sample mechanism is illustrated in Figure 3.1 this mechanism has 7 links $(n = 7)$, 7 turning pairs and 4 gear pairs $(k = 11)$. In each mechanism the number of links must be equal to the number of turning pairs. The labeling procedure of the T-T Graph method on the desired mechanism results in:

- 0 is assigned to the reference link.
- Links are numbered as 1, 2, 3, 4, 5, 6, and 7.

- Turning pairs are indicated by $\omega_{10}, \omega_{40}, \omega_{50}, \omega_{21}, \omega_{61}, \omega_{72}$, and ω_{32} labels.
- Gear meshes and related carrier arms are labeled by

$\omega'_{10}, \omega'_{40}, \omega''_{21}, \omega''_{51}, \omega'''_{62}, \omega'''_{72}, \omega''''_{72}$, and ω''''_{32}.

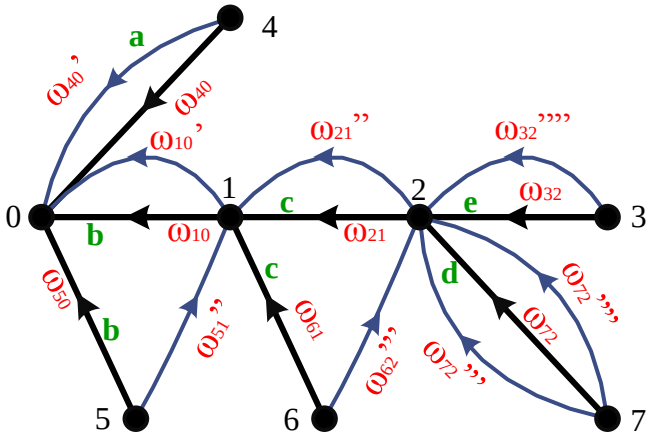

Figure 3.5: T-T graph of the mechanism.

In the following the paths (there exist more paths in this graph but for finding the transfer vertex, those paths where demonstrate the change in the level of axis location are considered) of the T-T graph, which is illustrated in Figure 3.5, are expressed so in this graph the transfer vertices are:

- Path 1 $(4 \xrightarrow{a} 0 \xrightarrow{b} 1)$: vertex 0 (pair axes *a*, *b*),
- Path 2 $(5 \xrightarrow{b} 0 \xrightarrow{b} 1 \xrightarrow{c} 2)$: vertex 1 (pair axes *b*, *c*),
- Path 3 $(6 \xrightarrow{c} 1 \xrightarrow{c} 2 \xrightarrow{d} 7)$: vertex 2 (pair axes *c*, *d*),
- Path 4 $(7 \xrightarrow{d} 2 \xrightarrow{e} 3)$: vertex 2 (pair axes *d*, *e*).

The sets of gear pair and corresponding carrier arm are $(4,1)(0)$, $(5,2)(1)$, $(6,7)(2)$, and $(7,3)(2)$ and the axis locations of the turning pairs are as follows:

- Axis *a*: pair $0-4$,

- Axis *c*: pairs $1-2$ and $1-6$,
- Axis *d*:pair $2-7$,
- Axis *e*: pair $2-3$.

As it was discussed above, the sample mechanism shown in Figure 3.1 contains four gear pairs. In a systematic way, the transfer vertices related to these gear pairs are acquired from Figure 3.5. As a result, following terminal equations, which express the angular velocities of the gears w.r.t. carrier arms, can be defined:

$$(4,1)(0):\omega'_{40}=-\frac{N_1}{N_4}\omega'_{10} \tag{3.53}$$

$$(5,2)(1):\omega''_{51}=-\frac{N_2}{N_5}\omega''_{21} \tag{3.54}$$

$$(6,7)(2):\omega'''_{62}=-\frac{N'_7}{N_6}\omega'''_{72} \tag{3.55}$$

$$(7,3)(2):\omega'''_{72}=\frac{N_3}{N''_7}\omega'''_{32} \tag{3.56}$$

As it was discussed in Section 2.3.3, by applying the right-hand-screw rule, the ratio is negative in the Eq. (3.53) to (3.55) since a positive rotation of input gear produces a negative rotation of output gear. While, in Eq. (3.56), ratio is positive because a positive rotation of input gear yields a positive rotation of output gear.

According to coaxial condition and Figure 3.5, it can be stated that:

$$\omega''_{51}=\omega_{50}-\omega_{10} \tag{3.57}$$

$$\omega'''_{62}=\omega_{61}-\omega_{21} \tag{3.58}$$

$$\omega'_{40}=\omega_{40} \tag{3.59}$$

$$\omega'_{10}=\omega_{10} \tag{3.60}$$

$$\omega''_{21} = \omega_{21} \tag{3.61}$$

$$\omega'''_{72} = \omega_{72} \tag{3.62}$$

$$\omega'''_{72} = \omega_{72} \tag{3.63}$$

$$\omega'''_{32} = \omega_{32} \tag{3.64}$$

It is observed that Eq. (3.57) to (3.64) are circuit equations which can be written from the graph directly and also Eq. (3.57) and (3.58) can be stated according to coaxial condition.

In the T-T graph shown in Figure 3.5, $\omega_{10}, \omega_{21}, \omega_{32}$, and ω_{72} are unknown angular velocities which can be obtained in terms of ω_{40}, ω_{50}, and ω_{61} as inputs by using Eq. (3.53) to (3.64). Eq. (3.53) to (3.56) indicate the inputs angular velocities in terms of output ones in gear pairs. In order to find unknown velocities in terms of inputs it is necessary to change the order of these equations by using Eq. (2.8):

$$\omega'_{10} = -N_{41}\omega'_{40} \tag{3.65}$$

$$\omega''_{21} = -N_{52}\omega''_{51} \tag{3.66}$$

$$\omega'''_{72} = -N_{67'}\omega'''_{62} \tag{3.67}$$

$$\omega'''_{32} = N_{7''3}\omega'''_{72} \tag{3.68}$$

where $N_{41} = \frac{N_4}{N_1}, N_{52} = \frac{N_5}{N_2}, N_{67'} = \frac{N_6}{N'_7}$ and $N_{7''3} = \frac{N''_7}{N_3}$.

Unknown velocities are obtained as follows:

Substituting Eq. (3.59) and (3.60) into Eq. (3.65) yields:

$$\omega_{10} = -N_{41}\omega_{40} \tag{3.69}$$

Substituting Eq. (3.57), (3.61) and (3.69) into Eq. (3.66) gives:

$$\begin{aligned}\omega_{21} &= -N_{52}(\omega_{50} - \omega_{10}) \\ &= -N_{52}\omega_{50} + N_{52}\omega_{10}\end{aligned}$$

$$\omega_{21} = -N_{52}\omega_{50} - N_{52}N_{41}\omega_{40} \tag{3.70}$$

Substituting Eq. (3.62), (3.58) and (3.70) into Eq. (3.67) results in:

$$\begin{aligned}\omega_{72} &= -N_{67'}(\omega_{61} - \omega_{21}) \\ &= -N_{67'}\omega_{61} + N_{67'}\omega_{21} \\ &= -N_{67'}\omega_{61} + N_{67'}(-N_{52}\omega_{50} - N_{52}N_{41}\omega_{40})\end{aligned}$$

$$\omega_{72} = -N_{67'}\omega_{61} - N_{67'}N_{52}\omega_{50} - N_{67'}N_{52}N_{41}\omega_{40} \tag{3.71}$$

Substituting Eq. (3.63), (3.64), and (3.71) into Eq. (3.68) yields:

$$\begin{aligned}\omega_{32} &= N_{7''3}\omega_{72} \\ &= N_{7''3}(-N_{67'}\omega_{61} - N_{67'}N_{52}\omega_{50} - N_{67'}N_{52}N_{41}\omega_{40})\end{aligned}$$

$$\omega_{32} = -N_{7''3}N_{67'}\omega_{61} - N_{7''3}N_{67'}N_{52}\omega_{50} - N_{7''3}N_{67'}N_{52}N_{41}\omega_{40} \tag{3.72}$$

In above equations, unknown angular velocities were defined in terms of inputs velocities and gear ratios. In the following, these velocities are indicated in the matrix form in terms of inputs and gear ratios:

$$\begin{pmatrix}\omega_{10}\\ \omega_{21}\\ \omega_{32}\\ \omega_{72}\end{pmatrix} = \begin{bmatrix} -N_{41} & 0 & 0 \\ -N_{52}N_{41} & -N_{52} & 0 \\ -N_{7''3}N_{67'}N_{52}N_{41} & -N_{7''3}N_{67'}N_{52} & -N_{7''3}N_{67'} \\ -N_{67'}N_{52}N_{41} & -N_{67'}N_{52} & -N_{67'}\end{bmatrix} \cdot \begin{pmatrix}\omega_{40}\\ \omega_{50}\\ \omega_{61}\end{pmatrix} \tag{3.73}$$

For better comparison of results in T-T Graph and Matroid, same notations are used for gear ratios as tooth ratios which were defined in Section 3.2.3.

$$i_{15} = N_{41},\ i_{16} = N_{52},\ i_{17} = N_{67'} \text{ and } i_{18} = N_{7''3} \tag{3.74}$$

$$\begin{pmatrix}\omega_{10}\\ \omega_{21}\\ \omega_{32}\\ \omega_{72}\end{pmatrix} = \begin{bmatrix} -i_{15} & 0 & 0 \\ -i_{16}i_{15} & -i_{16} & 0 \\ -i_{18}i_{17}i_{16}i_{15} & -i_{18}i_{17}i_{16} & -i_{18}i_{17} \\ -i_{17}i_{16}i_{15} & -i_{17}i_{16} & -i_{17}\end{bmatrix} \cdot \begin{pmatrix}\omega_{40}\\ \omega_{50}\\ \omega_{61}\end{pmatrix} \tag{3.75}$$

3.3.2 Denavit-Hartenberg (D-H) Convention

Up to here, kinematic analysis is done by using T-T Graph method and the unknown velocities are calculated in magnitude form. So by using these results and the D-H convention [56] more general analysis will be done in the following and unknown absolute velocities will be obtained in vectorial form rather than scalar form. Eq. (3.76) indicates the General Homogenous Transformation Matrix, ${}^{i-1}\mathbf{T}_i$, which is utilized as a tool for defining link i w.r.t link $i-1$ in the D-H convention:

$$
\begin{aligned}
{}^{i-1}\mathbf{T}_i &= \left[\begin{array}{c|c} {}^{i-1}\mathbf{R}_i & {}^{i-1}\mathbf{P}_i \\ \hline 0 & 1 \end{array}\right] \\
&= \left[\begin{array}{ccc|c} \cos\theta_{i,i-1} & -\sin\theta_{i,i-1}\cos\alpha_{i,i-1} & \sin\theta_{i,i-1}\sin\alpha_{i,i-1} & a_{i,i-1}\cos\theta_{i,i-1} \\ \sin\theta_{i,i-1} & \cos\theta_{i,i-1}\cos\alpha_{i,i-1} & -\cos\theta_{i,i-1}\sin\alpha_{i,i-1} & a_{i,i-1}\sin\theta_{i,i-1} \\ 0 & \sin\alpha_{i,i-1} & \cos\alpha_{i,i-1} & d_{i,i-1} \\ \hline 0 & 0 & 0 & 1 \end{array}\right]
\end{aligned}
\tag{3.76}
$$

As it is observed from Eq. (3.76), the ${}^{i-1}\mathbf{T}_i$ is made up of two submatrices: ${}^{i-1}\mathbf{R}_i$ which is 3×3 matrix indicating the orientation of link i w.r.t link $i-1$ and ${}^{i-1}\mathbf{P}_i$ which is 3×1 matrix indicating the position of link I w.r.t link $i-1$. Rotational submatrix is just used for kinematic analysis of sample mechanism so just ${}^{i-1}\mathbf{R}_i$ will be used instead of ${}^{i-1}\mathbf{T}_i$ as transformation matrix. D-H parameters, θ, d, a, and α, are introduced as follows:

- $\theta_{i,i-1}$: joint angle measured from x_{i-1} axis to x_i axis about z_{i-1} axis,
- $d_{i,i-1}$: translational displacement along z_{i-1} axis,
- $a_{i,i-1}$: joint offset length along common normal between z_{i-1} and z_i,
- $\alpha_{i,i-1}$: joint twist angle measured from z_{i-1} axis to z_i axis about x_{i-1} axis.

3.3.3 Equivalent Open-Loop Chain and Joint Coordinates

However, for dynamic analysis the entire functional schematic of mechanism must be considered because the mass center of the rigid body is important, it is sufficient that using equivalent open-loop chain for kinematic analysis since kinematic parameters are the same on the all points of the rigid body. This chain consists of the mechanical parts (i.e. turning pairs) which have effect on the orientation and position of the end-effector. Figure 3.6 indicates equivalent open-loop chain, which is used for defining joint coordinates, of the sample mechanism in Figure 3.1.

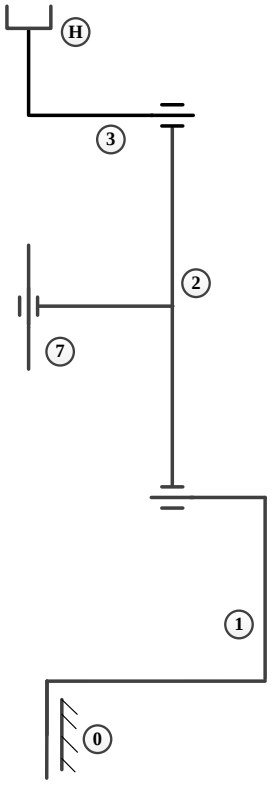

Figure 3.6: Equivalent open-loop chain of sample mechanism

According to Figure 3.6, joint coordinates can be defined. These coordinates are applied to the joints (turning pairs) and demonstrate the orientation of x-axes and z-axes, which are used in obtaining D-H parameters, of the joint. It is remarkable to mention that for open-loop chain shown in Figure 3.6, there exists a special case of joint coordinates for link 7 as it will be discussed in Section 3.3.5 and illustrated in

Figure 3.8. In Figure 3.7, joint coordinates which are applied for determining D-H parameters is illustrated. Also, these parameters are specified in Table 2.

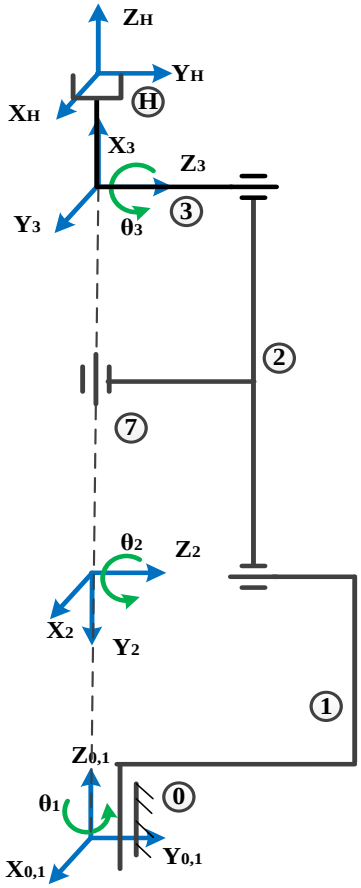

Figure 3.7: Joint coordinates used for end-effector

3.3.4 Applying D-H Convention

According to D-H convention and as shown in Figure 3.7, the sample mechanism shown in Figure 3.1 has three main joint variables. These joint variables are defined as follows:

- θ_1 :joint angle between link 1 w.r.t link 0 (θ_{10}),
- θ_2 :joint angle between link 2 w.r.t link 1 (θ_{21}),

- θ_3 : joint angle between link 3 w.r.t link 2 (θ_{32}).

Table 2: D-H parameters used for end-effector

	θ	d	a	α
1	θ_1	A_1	0	-90°
2	$\theta_2 - 90^\circ$	0	$A_3 - A_1$	0
3	$\theta_3 + 90^\circ$	0	0	$+90^\circ$

By inserting parameters from Table 2 into Eq. (3.76), all transformation matrices corresponding to Figure 3.7 can be determined as follows:

- Link 1 w.r.t link 0: $\theta_{10} = \theta_1$, $d_{10} = A_1$, $a_{10} = 0$, and $\alpha_{10} = -90^\circ$

$$ {}^0\mathbf{T}_1 = \begin{bmatrix} \cos\theta_1 & 0 & -\sin\theta_1 & 0 \\ \sin\theta_1 & 0 & \cos\theta_1 & 0 \\ 0 & -1 & 0 & A_1 \\ 0 & 0 & 0 & 1 \end{bmatrix} \tag{3.77} $$

- Link 2 w.r.t link 1: $\theta_{21} = \theta_2 - 90^\circ$, $d_{21} = 0$, $a_{21} = A_3 - A_1$, and $\alpha_{21} = 0$

$$ {}^1\mathbf{T}_2 = \begin{bmatrix} \sin\theta_2 & \cos\theta_2 & 0 & (A_3 - A_1)\sin\theta_2 \\ -\cos\theta_2 & \sin\theta_2 & 0 & -(A_3 - A_1)\cos\theta_2 \\ 0 & 0 & 1 & 0 \\ 0 & 0 & 0 & 1 \end{bmatrix} \tag{3.78} $$

Transformation matrix of link 2 w.r.t link 0 is produced by pre-multiplying Eq. (3.77) to Eq. (3.78):

$$ {}^0\mathbf{T}_2 = \begin{bmatrix} \cos\theta_1\sin\theta_2 & \cos\theta_1\cos\theta_2 & -\sin\theta_1 & (A_3 - A_1)\cos\theta_1\sin\theta_2 \\ \sin\theta_1\sin\theta_2 & \sin\theta_1\cos\theta_2 & \cos\theta_1 & -(A_3 - A_1)\sin\theta_1\sin\theta_2 \\ \cos\theta_2 & -\sin\theta_2 & 0 & (A_3 - A_1)\cos\theta_2 + A_1 \\ 0 & 0 & 0 & 1 \end{bmatrix} \tag{3.79} $$

- Link 3 w.r.t link 2: $\theta_{32} = \theta_3 + 90^\circ$, $d_{21} = 0$, $a_{21} = 0$, and $\alpha_{21} = +90^\circ$

$$ {}^{2}\mathbf{T}_{3} = \begin{bmatrix} -\sin\theta_3 & 0 & \cos\theta_3 & 0 \\ \cos\theta_3 & 0 & \sin\theta_3 & 0 \\ 0 & 1 & 0 & 0 \\ 0 & 0 & 0 & 1 \end{bmatrix} \tag{3.80} $$

Post-multiplying of Eq. (3.79) by Eq. (3.80) results in transformation matrix of link 3 w.r.t link2:

$$ {}^{0}\mathbf{T}_{3} = \begin{bmatrix} \cos\theta_1\cos(\theta_2+\theta_3) & -\sin\theta_1 & \cos\theta_1\sin(\theta_2+\theta_3) & (A_3-A_1)\cos\theta_1\sin\theta_2 \\ \sin\theta_1\cos(\theta_2+\theta_3) & \cos\theta_1 & \sin\theta_1\sin(\theta_2+\theta_3) & -(A_3-A_1)\sin\theta_1\sin\theta_2 \\ -\sin(\theta_2+\theta_3) & 0 & \cos(\theta_2+\theta_3) & (A_3-A_1)\cos\theta_2+A_1 \\ 0 & 0 & 0 & 1 \end{bmatrix} \tag{3.81} $$

As it was discussed at the first of Chapter 3, the GRM shown in Figure 3.1 has three input angular velocities (three DOF) as follows:

$$ \bar{\boldsymbol{\omega}}_{40} = \begin{pmatrix} 0 \\ 0 \\ \omega_{40} \end{pmatrix},\ \bar{\boldsymbol{\omega}}_{50} = \begin{pmatrix} 0 \\ 0 \\ \omega_{50} \end{pmatrix} \text{and}\ \bar{\boldsymbol{\omega}}_{61} = \begin{pmatrix} 0 \\ 0 \\ \omega_{61} \end{pmatrix} \tag{3.82} $$

These velocities are produced by θ_{40}, θ_{50}, and θ_{61} which are joint angles of link 4 w.r.t link 0, link 5 w.r.t link 0 and link 6 w.r.t link1 respectively. Eq. (3.82) illustrates these angular velocities in vectorial form and as it is observed, these inputs just have a component in their local z-axis. In other words, links 4, 5, and 6 just rotates about their local z-axis (i.e. joint angels of these links have just z-component w.r.t their local z-axis).

Figure 3.7 indicates unknown joint angles θ_i ($i = 1, 2, \text{and}, 3$). Unknown angular velocities $\bar{\boldsymbol{\omega}}_{10}$, $\bar{\boldsymbol{\omega}}_{21}$, and $\bar{\boldsymbol{\omega}}_{32}$ correspond to θ_1, θ_2, and θ_3 respectively. Note that, however in Section 3.2.4 $\bar{\boldsymbol{\omega}}_{72}$ was considered as an unknown angular velocity, it is not necessary to consider any unknown joint angle (unknown angular velocity) for link 7. Because this link is an intermediate link (gear) and it does not have any effect on the calculation of the end-effector's velocity. In fact, by referring to Figure 3.6, it

can be observed that just links 3, 2, and 1 (i.e. ${}^0\bar{\boldsymbol{\omega}}_{32}$, ${}^0\bar{\boldsymbol{\omega}}_{21}$, and ${}^0\bar{\boldsymbol{\omega}}_{10}$) have effect on the orientation and position of the end-effector. But for better comparison of methods, absolute velocity of link 7 will be obtained as it will be shown in Section 3.3.5 and θ_7 will be considered as the joint angle of this link. It is significant to mention that these unknown angular velocities have just z-component w.r.t their local z-axes as it is observed in Eq. (3.83).

$$\bar{\boldsymbol{\omega}}_{10}=\begin{pmatrix}0\\0\\\omega_{10}\end{pmatrix},\ \bar{\boldsymbol{\omega}}_{21}=\begin{pmatrix}0\\0\\\omega_{21}\end{pmatrix},\bar{\boldsymbol{\omega}}_{32}=\begin{pmatrix}0\\0\\\omega_{32}\end{pmatrix}\text{and}\,\bar{\boldsymbol{\omega}}_{72}=\begin{pmatrix}0\\0\\\omega_{72}\end{pmatrix} \tag{3.83}$$

In the following, by using ${}^{i-1}\mathbf{R}_i$ matrices as rotational submatrices of ${}^{i-1}\mathbf{T}_i$, which are defined above, and input angular velocities, first the unknown angular velocities will be obtained w.r.t reference frame and then all the links velocities can be obtained w.r.t base coordinate frame in the vectorial form:

$${}^0\bar{\boldsymbol{\omega}}_{10}=\bar{\boldsymbol{\omega}}_{10}=\begin{pmatrix}0\\0\\\omega_{10}\end{pmatrix} \tag{3.84}$$

It is clear that ${}^0\bar{\boldsymbol{\omega}}_{10}$ has just z-component w.r.t base since link 1 has just rotation about its local z-axis and this axis is parallel to the base z-axis.

$${}^0\bar{\boldsymbol{\omega}}_{21}={}^0R_1\cdot\bar{\boldsymbol{\omega}}_{21}=\begin{bmatrix}\cos\theta_1&0&-\sin\theta_1\\\sin\theta_1&0&\cos\theta_1\\0&-1&0\end{bmatrix}\cdot\begin{pmatrix}0\\0\\\omega_{21}\end{pmatrix}=\begin{pmatrix}-\sin\theta_1\omega_{21}\\\cos\theta_1\omega_{21}\\0\end{pmatrix} \tag{3.85}$$

Since just θ_1 has effect on orientation of ${}^0\bar{\boldsymbol{\omega}}_{21}$ and changes of this angle will change the orientation of ${}^0\bar{\boldsymbol{\omega}}_{21}$ in x_0y_0 plane so it has only *x* and *y* components w.r.t the base.

$$ {}^{0}\bar{\boldsymbol{\omega}}_{32} = {}^{0}R_{2} \cdot \bar{\boldsymbol{\omega}}_{32} = \begin{bmatrix} \cos\theta_1 \sin\theta_2 & \cos\theta_1 \cos\theta_2 & -\sin\theta_1 \\ \sin\theta_1 \sin\theta_2 & \sin\theta_1 \cos\theta_2 & \cos\theta_1 \\ \cos\theta_2 & -\sin\theta_2 & 0 \end{bmatrix} \cdot \begin{pmatrix} 0 \\ 0 \\ \omega_{32} \end{pmatrix} = \begin{pmatrix} -\sin\theta_1 \omega_{32} \\ \cos\theta_1 \omega_{32} \\ 0 \end{pmatrix} \quad (3.86) $$

It is obvious that θ_2 does not have any effect on ${}^{0}\bar{\boldsymbol{\omega}}_{32}$ and changes of this angle cannot make any change in the orientation of ${}^{0}\bar{\boldsymbol{\omega}}_{32}$. While, changes of θ_1 will change the orientation of ${}^{0}\bar{\boldsymbol{\omega}}_{32}$ in $x_0 y_0$ plane so it has only *x* and *y* components w.r.t the base.

In Eq. (3.84) to Eq. (3.86), the unknown angular velocities were calculated. In the rest, the links absolute velocities w.r.t the base will be obtained.

$$ \bar{\boldsymbol{\omega}}_{1}^{0} = {}^{0}\bar{\boldsymbol{\omega}}_{10} = \begin{pmatrix} 0 \\ 0 \\ \omega_{10} \end{pmatrix} = \begin{pmatrix} 0 \\ 0 \\ -i_{15}\omega_{40} \end{pmatrix} \quad (3.87) $$

$$ \bar{\boldsymbol{\omega}}_{2}^{0} = {}^{0}\bar{\boldsymbol{\omega}}_{21} + {}^{0}\bar{\boldsymbol{\omega}}_{10} = \begin{pmatrix} -\sin\theta_1 \omega_{21} \\ \cos\theta_1 \omega_{21} \\ 0 \end{pmatrix} + \begin{pmatrix} 0 \\ 0 \\ \omega_{10} \end{pmatrix} = \begin{pmatrix} -\sin\theta_1 \omega_{21} \\ \cos\theta_1 \omega_{21} \\ \omega_{10} \end{pmatrix} $$

$$ = \begin{pmatrix} -\sin\theta_1 (-i_{16} i_{15} \omega_{40} - i_{16} \omega_{50}) \\ \cos\theta_1 (-i_{16} i_{15} \omega_{40} - i_{16} \omega_{50}) \\ -i_{15}\omega_{40} \end{pmatrix} \quad (3.88) $$

$$ \bar{\boldsymbol{\omega}}_{3}^{0} = {}^{0}\bar{\boldsymbol{\omega}}_{32} + {}^{0}\bar{\boldsymbol{\omega}}_{21} + {}^{0}\bar{\boldsymbol{\omega}}_{10} = \begin{pmatrix} -\sin\theta_1 \omega_{32} \\ \cos\theta_1 \omega_{32} \\ 0 \end{pmatrix} + \begin{pmatrix} -\sin\theta_1 \omega_{21} \\ \cos\theta_1 \omega_{21} \\ 0 \end{pmatrix} + \begin{pmatrix} 0 \\ 0 \\ \omega_{10} \end{pmatrix} = \begin{pmatrix} -\sin\theta_1 (\omega_{32} + \omega_{21}) \\ \cos\theta_1 (\omega_{32} + \omega_{21}) \\ \omega_{10} \end{pmatrix} $$

$$ = \begin{pmatrix} -\sin\theta_1 (-i_{16} i_{15} (i_{18} i_{17} + 1)\omega_{40} - i_{16}(i_{18} i_{17} + 1)\omega_{50} - i_{18} i_{17} \omega_{61}) \\ \cos\theta_1 (-i_{16} i_{15} (i_{18} i_{17} + 1)\omega_{40} - i_{16}(i_{18} i_{17} + 1)\omega_{50} - i_{18} i_{17} \omega_{61}) \\ -i_{15}\omega_{40} \end{pmatrix} \quad (3.89) $$

In Eq. (3.88) and Eq. (3.89), if the rest position $(\theta_1 = 0)$ is considered, the results in these equations will be the same as the results in Eq. (3.47) and Eq. (3.48) respectively.

3.3.5 Different Case of Link 7

Since the end-effector in the desired mechanism is attached to the link 3, it will be adequate to obtain the velocity of the link 3. As it was mentioned in Section 3.3.4 and according to Eq. (3.89), angular velocity of link 3 is made up of ${}^0\bar{\boldsymbol{\omega}}_{32}$, ${}^0\bar{\boldsymbol{\omega}}_{21}$, and ${}^0\bar{\boldsymbol{\omega}}_{10}$. Hence, it is well observed that link 7 has not any effect on velocity of end-effector. Figure 3.1 illustrates that link 7 is just used as an intermediate link to transfer input angular velocity from *M3* to link 3. Therefore, the z-axis of the link 3 w.r.t. link 2 is parallel to the z-axis of link 2 w.r.t. link 1. As a result, in all of possible cases of displacements of the mechanism's links these to z-axes are parallel to each other (as indicated in Figure 3.7). Though these two z-axes are parallel, the z-axis of the link 7 w.r.t. link 2 is perpendicular to them. That is, there exists $+90^\circ$ twist angle from z-axis of link 2 to z-axis of link 7 and -90° twist angle from z-axis of link 7 to link 3 (as indicated in Figure 3.8 and Table 3). This is the main reason to consider different joint coordinates and D-H parameters for link 7 as defined in Figure 3.8 and Table 3.

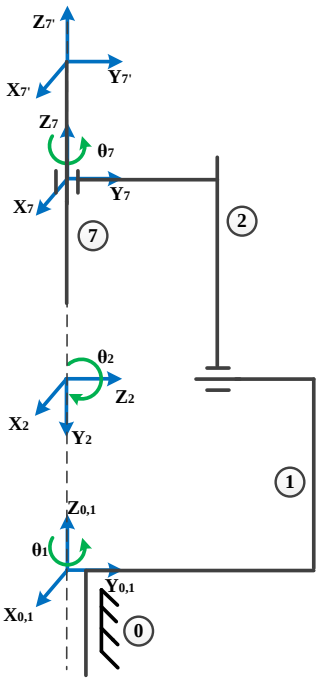

Figure 3.8: Joint coordinates used for link 7

Consequently, by referring to Figure 3.5, it can be noticed that the angular velocity of link 7 w.r.t. 0 ($\bar{\boldsymbol{\omega}}_7^0$) is comprised of ${}^0\bar{\boldsymbol{\omega}}_{72}$, ${}^0\bar{\boldsymbol{\omega}}_{21}$, and ${}^0\bar{\boldsymbol{\omega}}_{10}$. ${}^0\bar{\boldsymbol{\omega}}_{10}$ is same as Eq. (3.84) since z-axis of link 1 is parallel to z-axis of the base and ${}^0\bar{\boldsymbol{\omega}}_{21}$ is same as Eq. (3.85) since same D-H parameters in both Table 2 and Table 3 are used in obtaining ${}^0\mathbf{R}_1$. Thus, it will be sufficient to pre-multiplying ${}^1\mathbf{R}_2$ by $\bar{\boldsymbol{\omega}}_{72}$ to obtain ${}^0\bar{\boldsymbol{\omega}}_{72}$ as follows:

Table 3: D-H parameters used for link 7

	θ	d	a	α
1	θ_1	A_1	0	-90°
2	θ_2	$A_2 - A_1$	0	$+90^\circ$
7	θ_7	d_z	0	0

- Link 1 w.r.t link 0: $\theta_{10} = \theta_1$, $d_{10} = A_1$, $a_{10} = 0$, and $\alpha_{10} = -90^\circ$

$$ {}^0\mathbf{T}_1 = \begin{bmatrix} \cos\theta_1 & 0 & -\sin\theta_1 & 0 \\ \sin\theta_1 & 0 & \cos\theta_1 & 0 \\ 0 & -1 & 0 & A_1 \\ 0 & 0 & 0 & 1 \end{bmatrix} \tag{3.90} $$

- Link 2 w.r.t. link 0: $\theta_{21} = \theta_2$, $d_{21} = A_2 - A_1$, $a_{21} = 0$, and $\alpha_{21} = +90^\circ$

$$ {}^1\mathbf{T}_2 = \begin{bmatrix} \cos\theta_2 & 0 & -\sin\theta_2 & 0 \\ \sin\theta_2 & 0 & \cos\theta_2 & 0 \\ 0 & 1 & 0 & A_2 - A_1 \\ 0 & 0 & 0 & 1 \end{bmatrix} \tag{3.91} $$

Pre-multiplying Eq. (3.91) by Eq. (3.90) yields transformation matrix of link 2 w.r.t link 0:

$$ {}^{0}\mathbf{T}_{2} = \begin{bmatrix} \cos\theta_1\cos\theta_2 & -\sin\theta_1 & \cos\theta_1\sin\theta_2 & -(A_2 - A_1)\sin\theta_1 \\ \sin\theta_1\sin\theta_2 & \cos\theta_1 & \sin\theta_1\sin\theta_2 & (A_2 - A_1)\cos\theta_1 \\ -\sin\theta_2 & 0 & \cos\theta_2 & A_1 \\ 0 & 0 & 0 & 1 \end{bmatrix} \tag{3.92} $$

- Link 7 w.r.t link 2: $\theta_{72} = \theta_7$, $d_{21} = d_z$, $a_{21} = 0$, and $\alpha_{21} = 0$

$$ {}^{2}\mathbf{T}_{7} = \begin{bmatrix} \cos\theta_7 & -\sin\theta_7 & 0 & 0 \\ \sin\theta_7 & \cos\theta_7 & 0 & 0 \\ 0 & 0 & 1 & d_z \\ 0 & 0 & 0 & 1 \end{bmatrix} \tag{3.93} $$

Post-multiplying Eq. (3.92) by Eq. (3.93) results in transformation matrix of link 7 w.r.t link 0:

$$ {}^{0}\mathbf{T}_{7} = \begin{bmatrix} \cos\theta_1\cos\theta_2\cos\theta_7 - \sin\theta_1\sin\theta_7 & -\sin\theta_1\cos\theta_7 - \cos\theta_1\cos\theta_2\sin\theta_7 & \cos\theta_1\sin\theta_2 & \sin\theta_1(A_2 - A_1) + d_z\cos\theta_1\sin\theta_2 \\ \sin\theta_1\cos\theta_2\cos\theta_7 + \cos\theta_1\sin\theta_7 & \cos\theta_1\cos\theta_7 - \sin\theta_1\cos\theta_2\sin\theta_7 & \sin\theta_1\sin\theta_2 & d_z\sin\theta_1\sin\theta_2 - \cos\theta_1(A_2 - A_1) \\ -\sin\theta_2\cos\theta_7 & \sin\theta_2\sin\theta_7 & \cos\theta_2 & A_1 d_z\cos\theta_2 \\ 0 & 0 & 0 & 1 \end{bmatrix} $$

(3.94)

By using ${}^{0}\mathbf{R}_{2}$ which is rotational sub-matrix of Eq. (3.92) and pre-multiplying it by $\bar{\boldsymbol{\omega}}_{72}$ from Eq. (3.83), first ${}^{0}\bar{\boldsymbol{\omega}}_{72}$ and then $\bar{\boldsymbol{\omega}}_{7}^{0}$ will be obtained as follows:

$$ {}^{0}\bar{\boldsymbol{\omega}}_{72} = {}^{0}R_{2}\cdot\bar{\boldsymbol{\omega}}_{72} = \begin{bmatrix} \cos\theta_1\cos\theta_2\cos\theta_7 - \sin\theta_1\sin\theta_7 & -\sin\theta_1\cos\theta_7 - \cos\theta_1\cos\theta_2\sin\theta_7 & \cos\theta_1\sin\theta_2 \\ \sin\theta_1\cos\theta_2\cos\theta_7 + \cos\theta_1\sin\theta_7 & \cos\theta_1\cos\theta_7 - \sin\theta_1\cos\theta_2\sin\theta_7 & \sin\theta_1\sin\theta_2 \\ -\sin\theta_2\cos\theta_7 & \sin\theta_2\sin\theta_7 & \cos\theta_2 \end{bmatrix} \cdot \begin{pmatrix} 0 \\ 0 \\ \omega_{72} \end{pmatrix} = \begin{pmatrix} (\cos\theta_1\sin\theta_2)\omega_{72} \\ (\sin\theta_1\sin\theta_2)\omega_{72} \\ (\cos\theta_2)\omega_{72} \end{pmatrix} $$

(3.95)

$$ \bar{\boldsymbol{\omega}}_{7}^{0} = {}^{0}\bar{\boldsymbol{\omega}}_{72} + {}^{0}\bar{\boldsymbol{\omega}}_{21} + {}^{0}\bar{\boldsymbol{\omega}}_{10} = \begin{pmatrix} \cos\theta_1\sin\theta_2\omega_{72} \\ \sin\theta_1\sin\theta_2\omega_{72} \\ \cos\theta_2\omega_{72} \end{pmatrix} + \begin{pmatrix} -\sin\theta_1\omega_{21} \\ \cos\theta_1\omega_{21} \\ 0 \end{pmatrix} + \begin{pmatrix} 0 \\ 0 \\ \omega_{10} \end{pmatrix} = \begin{pmatrix} \cos\theta_1\sin\theta_2\omega_{72} - \sin\theta_1\omega_{21} \\ \sin\theta_1\sin\theta_2\omega_{72} + \cos\theta_1\omega_{21} \\ \cos\theta_2\omega_{72} + \omega_{10} \end{pmatrix} $$

$$ = \begin{pmatrix} -i_{16}\left(\cos\theta_1\sin\theta_2 i_{17} - \sin\theta_1\right)\left(i_{15}\omega_{40} + \omega_{50}\right) - \cos\theta_1\sin\theta_2 i_{17}\omega_{61} \\ -i_{16}\left(\sin\theta_1\sin\theta_2 i_{17} + \cos\theta_1\right)\left(i_{15}\omega_{40} + \omega_{50}\right) - \sin\theta_1\sin\theta_2 i_{17}\omega_{61} \\ -i_{15}\left(\cos\theta_2 i_{17} i_{16} + 1\right)\omega_{40} - \cos\theta_2 i_{17} i_{16}\omega_{50} - \cos\theta_2 i_{17}\omega_{61} \end{pmatrix} \tag{3.96} $$

By considering the rest position i.e. $\theta_1 = \theta_2 = 0$, the results in Eq. (3.96) will be the same as the results in Eq. (3.52).

Chapter 4

CONCLUSIONS

4.1 Conclusions

In this thesis Matroid and T-T Graph methods, which are based on Graph Theory are considered for the kinematic analysis of geared robotic mechanism. Both methods use directed graphs. In Matroid method, links are represented by nodes (vertices) and revolute pairs and gear pairs are represented by bold and dash lines, respectively. The graph lines show only the kinematic structure of the mechanism and do not carry any other information. The incident and path matrices are obtained from the graph and cycle bases matrix is derived from these matrices. On the other hand, each line in T-T graph represents the terminal graph of the joint or gear pairs and therefore carries a pair of information (angular velocity and torque). The fundamental circuit or fundamental cut-set equations can be obtained from the T-T graph very easily.

Matroid method, on the one hand, by combining Graph Theory and Algebra yields a long procedure since a number of matrices must be acquired. On the other hand, these matrices can be used for expressing any mechanism in more details. This method would be able to find the correct sign of teeth ratio (i.e. positive or negative sign) in a systematic way by using cycle matrix and pitch diameters. Matroid method does not use transfer vertex and therefore the determination of this vertex is not important in this method. In fact, the cycle bases in matroid are defined directly from associated graph and f-circuit equations are written from upper vector in dual vector

while these equations are not used in any step of analysis. By contrast, In T-T method, in order to write the terminal equations of the gear pairs, the transfer vertices should be determined by labeling the rotation axes. By using terminal equations and f-circuit equations, which are obtained from the graph, the kinematic equations of the mechanism are obtained. Determination of teeth ratio's sign is the main challenge of T-T because this sign is determined according to rotation of output link w.r.t. input link by using right-hand-screw. Finding correct sign of teeth ratio is so important since this ratio has effect in terminal equation. If the sign was not determined correctly, there exists a sign problem in final results. T-T method, however, not only is useful for modeling and analyzing of robotics mechanisms but also can be used to model and analyze any physical and dynamical systems. This is the main advantage of T-T method.

Since some of the velocities in the geared robotic mechanism are not scalar and they are vectorial quantities, Matroid uses Plücker coordinates and Screw theory to determine these quantities. On the other hand T-T method uses either Network Model Approach developed by Tokad or D-H convention. D-H convention was used in this thesis. If the results of D-H convention and Matroid method are compared, it is seen than Matroid method obtains the kinematic equations of the mechanisms in rest position ($\theta_1 = 0$ and for special case $\theta_1 = \theta_2 = 0$). However, the equations obtained from the D-H conventions are more general. That means, all possible rotations and positions of the mechanism are considered.

4.2 Future Works

As it was mentioned above, determining the sign of the gear ratio is a significant challenge in T-T Graph Method. In Matroid the sign of this ratio will be obtained

systematically according to Cycle-Basis matrix and gears' diameter whereas in another method this determination must be done according to Right-Hand-Screw rule manually. As a result, T-T Graph Method can be developed by inserting a systematic procedure in which the sign of gear ratio is determined. T-T Graph method not only can be considered as a powerful graphical method in kinematic and dynamic analysis of geared systems but also it will be able to speed up computer algorithms, which are used in modeling and simulation, if we can modify its challange. Hence, developing and applying this method as computer aided approach can be regarded as another future work.

REFERENCES

[1] R. Willis, *Principles of Mechanism*, 2nd ed., London: Longmans, Green and Co., 1870.

[2] G. H. Martin, *Kinematics and Dynamics of Machines*, New York: McGraw-Hill, 1969, p. 298–306.

[3] W. L. Cleghorn and G. Tyc, "Kinematic Analysis of Planetary Gear Trains Using a Microcomputer," *Int. J. Mech. Eng. Educ.*, vol. 15, p. 57–69, 1987.

[4] R. L. Norton, *Design of Machinery*, New York: McGraw-Hill, 2004, pp. 497-499.

[5] R. J. Willis, "On the Kinematics of the Closed Epicyclic Differential Gears," *ASME Journal of Mechanical Design*, vol. 104, pp. 712-723, 1982.

[6] D. Gibson and S. Kramer, "Symbolic Notation and Kinematic Equations of Motion of the Twenty-Two Basic Spur, Planetary Gear Trains," *ASME Journal of Mechanisms, Transmissions and Automation in Design*, vol. 106, pp. 333-340, 1984.

[7] J. Uicker Jr., “Displacement Analysis of Spatial Mechanisms by an Iterative Method Based on 4x4 Matrices”, M.S. Thesis, Northwestern University

Evanston, Illinois, June 1963.

[8] P. Nikravesh, R. Wehage and O. Kwon, "Euler Parameters in Computational Kinematics and Dynamics, Part 1 and Part 2," *ASME Journal of Mechanisms, Transmissions, and Automation in Design*, vol. 107, no. 1, pp. 358-365, March 1985.

[9] J. Shigley and J. Uicker Jr., *Theory of Machines and Mechanisms*, New York: McGraw-Hill, 1980.

[10] J. Wojnarowski and A. Lidwin, "The Application of Signal Flow Graphs to the Kinematic Analysis of Planetary Gear Trains," *Mechanism and Machine Theory*,vol. 10, no. 1-B, pp. 17-31, 1975.

[11] D. Karnopp and R. Rosenberg, *System Dynamics, Modelling and Simulation of Mechatronic Systems*, New York: J. Wiley, 1975.

[12] Y. Hu, "Application of Bond Graphs and Vector Bond Graphs to Rigid Body Dynamics," *Journal of China Textile University (English Edition)*, vol. 5, no. 4, pp. 67-75, 1988.

[13] J. Choi and M. Bryant, "CombiningLlumped Parameter Bond Graphs with Finite Element Shaft in A Gear Box Model," *Computer Modeling in Engineering and Science*, vol. 3, no. 4, pp. 431-446, 2002.

[14] F. Buchsbaum and F. Freudenstein, "Synthesis of Kinematic Structure of Geared Kinematic Chains and Other Mechanisms," *Journal of Mechanisms*, vol. 5, no. 3, pp. 357-392, 1970.

[15] F. Freudenstein and A. Yang, "Kinematics and Statics of A Coupled Epicyclic Spur-Gear Train," *Mechanism and Machine Theory*, vol. 7, no. 2, pp. 263-275, 1972.

[16] C. Hsu, "Graph Notation for the Kinematic Analysis of Differential Gear Trains," *Joumal of the Franklin Institute*, vol. 329, no. 5, pp. 859-867, 1992.

[17] C. Hsu, "Graph Representation for the Structural Synthesis of Geared Kinematic Chains," *Journal of the Franklin Institute*, vol. 330, no. 1, pp. 131-143, 1993.

[18] C. Hsu and K. Lam, "Automatic Analysis of Kinematic Structure of Planetary Gear Trains," *ASME Journal of Mechanical Design*, vol. 115, no. 3, pp. 631-638, 1993.

[19] H. Hsieh and L. Tsai, "Kinematic Analysis of Epicyclic-Type Transmission Mechanisms Using the Concept of Fundamental Geared Entities," *ASME Journal of Mechanical Design*, vol. 118, no. 2, pp. 294-299, 1996.

[20] C. Hsu and Y. Wu, "Automatic Detection of Embedded Structure in Planetary Gear Trains," *Journal of Mechanical Design, Transactions of the ASME*, vol.

119, no. 2, pp. 315-318, 1997.

[21] S. Lang, "Graph-Theoretic Modeling of Epicyclic Gear Systems," *Mechanism and Machine Theory*, vol. 40, pp. 511-529, 2005.

[22] F. Freudenstein, "Application of Boolean Algebra to the Motion of Epicyclic Drives," *ASME Journal of Engineering for Industry*, vol. 93, no. 1, pp. 176-182, February 1972.

[23] L. Tsai, "An Application of Graph Theory to the Detection of Fundamental Circuits in Epicyclic Gear Trains," Technical Report T.R. 95-97, Institute for Systems Research, College Park, Maryland, 1995.

[24] W. Sohn and F. Freudenstein, "An Application of Dual Graphs to the Automatic Generation of the Kinematic Structures of Mechanisms," *ASME Journal of Mechanisms, Transmissions, and Automation in Design*, vol. 108, pp. 392-398, 1986.

[25] L. Tsai, "An Algorithm for the Kinematic Analysi of Epicyclic Gear Trains," in *Proc. of the 9th Applied Mechanisms Conf.*, Kansas City, 1985.

[26] A. Hedman, "Transmission Analysis, Automatic Derivation of Relationships," *ASME Journal of Mechanical Design*, vol. 115, no. 4, pp. 1031-1037, 1993.

[27] A. Rao, "A Genetic Algorithm for Topological Characteristics of Kinematic Chains," *ASME Journal of Mechanical design*, vol. 122, pp. 228-231, 2000.

[28] S. Zawislak, "Artificial Intelligence Aided Design of Gears," in *12th IFToMM World Congress*, Besançon (France), 2007.

[29] M. Zhang, N. Liao and C. Zhou, "A Modified Hopfield Neuronal Networks Model for Graphs-Based Kinematic Structure Design," *Engineering with Computers*, vol. 26, pp. 75-80, 2010.

[30] T. Mruthyunjaya and M. Raghavan, "Structural Analysis of Kinematic Chains and Mechanisms Based on Matrix Representation," *ASME Journal of Mechanical Design*, vol. 101, pp. 488-494, 1979.

[31] G. Chatterjee and L. Tsai, "Computer-Aided Sketching of Epicyclic-Type Automatic Transmission Gear Trains," *ASME Journal of Mechanical Design*, vol. 118, no. 3, pp. 405-411, 1996.

[32] L. Tsai, *Mechanisms design. Enumeration of kinematic structures according to function*, Boca Raton, Florida: CRC Press, 2000.

[33] A. Yang and F. Freudenstein, "Mechanics of Epicyclic Bevel-Gear Trains," in *Mechanisms Conference*, San Francisco, 1972.

[34] F. Freudenstein, R. Longman and C. Chen, "Kinematic Analysis of Robotic Bevel-Gear Trains," *ASME Journal of Mechanisms, Transmissions, and Automation in Design*, vol. 106, pp. 371-375, September 1984.

[35] L. Tsai, "The Kinematics of Spatial Robotic Bevel-Gear Trains," *IEEE Journal of Robotics and Automation*, vol. 4, no. 2, pp. 150-156, April 1988.

[36] Anonymous, "Bevel Gears Make Robot's "Wrist" More Flexible," *Machine Design*, vol. 54, no. 18, p. 55, August 1982.

[37] C. Day, H. Akeel and L. Gutkowski, "Kinematic Design and Analysis of Coupled Planetary Bevel-Gear Trains," *ASME Journal of Mechanisms, Transmissions and Automation in Design*, vol. 105, no. 3, pp. 441-445, September 1983.

[38] R. Ma and K. Gupta, "On the Motion of Oblique Bevel Geared Robot Wrists," *Journal of Robotic Systems*, vol. 5, pp. 509-520, 1989.

[39] F. Litvin and Y. Zheng, "Robotic bevel-gear differential train," *International Journal of Robotics*, vol. 5, no. 2, pp. 75-81, 1986.

[40] M. Uyguroğlu and Y. Tokad, "'Kinematic analysis of robotic bevel-gear trains: An application of network model approach," *Meccanica*, vol. 33, pp. 177-194, 1998.

[41] S. Chang, “Redundant-Drive Backlash-Free Robotic Mechanisms: Mechanisms Creation, Analysis, and Control”, Ph.D. Dissertation, University of Maryland, College Park, Maryland, 1991.

[42] J. Oxley, *Matroid Theory*, Oxford: Oxford University Press, 1992.

[43] N. White, *Theory of Matroids*, Cambridge: Cambridge University Press, 1986.

[44] H. Whitney, "On the Abstract Properties of Linear Dependence," *American Journal of Mathematics*, vol. 57, pp. 509-533, 1935.

[45] O. Shai, "The Multidisciplinary Combinatorial Approach and its Applications in Engineering," *Artif. Intell. Eng. Des. Anal. Manuf.*, vol. 15, pp. 109-144, 2001.

[46] I. Talpasanu, T. Yih and P. Simionescu, "Application of Matroid Method in Kinematic Analysis of Parallel Axes Epicyclic Gear Trains," *ASME Journal of Mechanical Design*, vol. 128, pp. 1307-1314, 2006.

[47] I. Talpasanu and P. Simionescu, "Kinematic Analysis of Epicyclic Bevel Gear Trainns With Matroid Method," *ASME Journal of Mechanical Design*, vol. 134, pp. 1-8, 2012.

[48] I. Talpasanu and P. Murty, "Open Chain Systems Based on Oriented Graph-Matroid Theory," *SAE Int. J. Passeng. Cars - Mech. Syst.,* vol. 1, no. 1, pp. 189-

199, 2009.

[49] I. Talpasanu, “Kinematics and Dynamics of Mechanical Systems Based on Graph-Matroid Theory”, Ph.D. Dissertation, University of Texas at Arlington, Arlington, Texas, 2004.

[50] M. Uyguroğlu and H. Demirel, "TSAI–TOKAD (T–T) Graph: The Combination of Non-oriented and Oriented Graphs for the Kinematics of Articulated Gear Mechanisms," *Meccanica*, vol. 40, pp. 223-232, 2005.

[51] M. Uyguroğlu and H. Demirel, "Kinematic analysis of tendon-driven robotic mechanisms using oriented graphs," *Acta Mechanica*, vol. 182, pp. 265-277, 2006.

[52] H. Koenig, Y. Tokad and H. Kesevan, *Analysis of Discrete Physical Systems*, New York: McGraw-Hill, 1967.

[53] J. Chou, H. Kesevan and K. Singhal, "A systems approach to three-dimensional multibody systems using graph-theoretical model," *IEEE Transactions on Systems, Man, and Cybernetics*, vol. 16, no. 2, pp. 219-230, 1986.

[54] Y. Tokad, "A network model for rigid-body motion," *Dynamics Control*, vol. 2, no. 1, pp. 59-82, 1992.

[55] R. Ball, *Treatise on the Theory of Screws*, Cambridge, England: Cambridge University Press, 1998.

[56] R. Hartenberg and J. Denavit, *Kinematic synthesis of linkages*, New York: McGraw-Hill, 1964.